

Functional L-Optimality Subsampling for Massive Data

Hua Liu

Department of Statistics and Management, Shanghai University of Finance and Economics, Shanghai, China.

E-mail: liuhua_sufe@163.com

Jinhong You

Department of Statistics and Management, Shanghai University of Finance and Economics, Shanghai, China.

E-mail: johnyou07@163.com

Jiguo Cao

Department of Statistics and Actuarial Science, Simon Fraser University, BC, Canada.

E-mail: jiguo.cao@gmail.com

Summary. Massive data bring the big challenges of memory and computation to researchers, which can be tackled to some extent by taking subsamples from the full data as a surrogate. For functional data, it is common to collect measurements intensively over their domains, which require more memory and computation time when the sample size is large. The situation would be much worse when the statistical inference is made through bootstrap samples. To the best of our knowledge, there is no work to study the subsampling for the functional linear regression or its generation systematically. In this article, based on the functional L-optimality criterion we propose an optimal subsampling method for the functional linear model. When the response is a discrete or categorical variable, we further extend this subsampling method to the functional generalized linear model. We establish the asymptotic properties of the resultant estimators by the subsampling methods. The finite sample performance of our proposed subsampling methods is investigated by extensive simulation studies. We also apply our proposed subsampling methods to analyze the global climate data and the kidney transplant data. The results from the analysis of these data show that the optimal subsampling methods motivated by the functional L-optimality criterion are much better than the uniform subsampling method and can well approximate the results based on full data.

Keywords: Functional regression, Functional L-optimality, Massive data, Penalized B-spline, Subsampling

1. Introduction

In the past decade, the volume of data increases exponentially with the development of science and technology, which provides researchers more information. At the same time, despite the rapid development of computational resources, the extraordinary amount of data also brings some challenges to researchers in conducting data analysis. One challenge is that fitting a model using massive data needs too much memory and exceeds

the maximum capacity of a single computer. Moreover, the computing time may be too long to obtain the results. To tackle these challenges, an effective way is to take random subsamples from the massive data as a surrogate.

The existing literature about subsampling mainly focuses on the models with scalar variables. For a linear regression, [Ma et al. \(2015\)](#) used the probabilities based on statistical leverage scores to randomly subsample data and established the asymptotic properties of the resultant estimators. Besides, a method named information-based optimal subdata selection (IBOSS) proposed by [Wang et al. \(2019\)](#) selects subsample data deterministically without involving random sampling. For a logistic regression, [Wang et al. \(2018a\)](#) proposed a subsampling method based on the A-optimality criterion, [Wang \(2019\)](#) proposed a Poisson subsampling method ([Kiefer, 1959](#)) based on the subsamples taken according to the optimal subsampling probabilities developed in [Wang et al. \(2018a\)](#) and [Cheng et al. \(2020\)](#) used the IBOSS method to make subsampling. [Ai et al. \(2021b\)](#) investigated the optimal subsampling method under the A-optimality criterion (OSMAC) for generalized linear models. A Poisson subsampling method based on the A-optimality or L-optimality criterion was used for maximum quasi-likelihood estimation in ([Yu et al., 2020a](#)). [Wang and Ma \(2021\)](#), [Fan et al. \(2021\)](#) and [Ai et al. \(2021a\)](#) used the subsampling method for quantile regressions. We refer the readers to [Yao and Wang \(2021\)](#) for a recent review of optimal subsampling methods of massive data when both of the response and predictors are scalar.

It is worth mentioning that there is almost no work to study the functional regressions in the field of subsampling systematically. However, in applications, especially in the clinical, biometrical, epidemiological, social and economic fields, many variables are measured or observed at multiple times or positions. This kind of variable is therefore called a functional variable, and the data for the variable are called functional data ([Ramsay and Silverman, 2002](#); [Morris, 2015](#)). One of the most important functional regressions is the functional linear model, which describes the relationship of some functional covariates and scalar responses ([Cardot et al., 1999, 2003](#); [Hall and Horowitz, 2007](#); [Hilgert et al., 2013](#); [Jiang and Wang, 2011](#); [Jiang et al., 2020](#); [Li and Zhu, 2020](#)).

For the functional linear model, the time complexity of the penalized B-splines method ([Cardot et al., 2003](#); [Claeskens et al., 2009](#); [Xiao et al., 2019](#)) is $O(n + n(K + p + 1)^2)$, where n is the sample size, K is the number of knots and p is the degree of the spline. Usually, K is chosen to be relatively large to capture the local features of the functions. Moreover, each sample has multiple measurements in the domain, and sometimes the number of observations may even be very large in the functional data. Thus, when the sample size is extremely large, we have to face more serious challenges than mentioned above, especially we also need to select the optimal smoothing parameter by the Bayesian information criterion (BIC). For example, the global climate data record the daily maximum temperature, daily minimum temperature and daily precipitation from January 1st, 1950 to December 30th, 2100 of all 1,036,800 grids in the globe. The data can be used to analyze the changes in the global climate during the past few decades and study the future trend of global change. The data size of the whole global climate data during 1950-2100 is above 1TB, which is too large to be held in the most common computers. Thus, the statistical analysis based on the full data is difficult. Another example is about the kidney transplant data from the Organ Procurement Transplant Network/United

Network for Organ Sharing (Optrn/UNOS). This data set collects the information of 478,380 recipients during the follow-up period, which can be used to identify whether the transplant is successful. For the above classification problem, we need to use an iterative procedure to get the estimator, thus, the computation requires too long to get the results when the full data is used.

We consider using the idea of subsampling to solve the challenges in the computation with functional covariates. The simplest subsampling method is to draw the sample uniformly at random, which will perform poorly when the leverage scores are non-uniform. Also, to make the B-spline approximation bias asymptotically negligible, a relatively large K is usually chosen. Simultaneously, a roughness penalty is also usually used to ensure the smoothness of the estimator, which results in the variance of the subsample estimator being more complicated and not as concise as that in Wang et al. (2019) and Cheng et al. (2020). Thus, the deterministic selection method (IBOSS) (Wang et al., 2019; Cheng et al., 2020) seems to not be suitable for the subsampling with functional covariates.

In this paper, first, we estimate the coefficient functions using the subsampling data, and derive the asymptotic distribution of the general subsampling estimator. Then, we get the optimal subsampling probabilities based on the asymptotic integrated mean squared errors (IMSE) and the proposed functional L-optimality criterion. Lastly, we obtain the optimal subsampling estimator based on the optimal subdata drawn according to the optimal probability calculated above. Besides, to make the computation more efficient, we choose sampling with replacement rather than sampling without replacement.

To the best of our knowledge, this is the first attempt to introduce the subsampling method to the functional data analysis. And the optimal subsampling method based on functional L-optimality has several advantages : (1) the computing time for this method is $O(n + (L_0 + L) * (K + p + 1)^2)$ with the subsample size L_0 and L , which is significantly faster than using the full data $O(n + n(K + p + 1)^2)$; (2) the integrated mean square errors (IMSEs) of the resultant estimators using this method are smaller than those using uniform subsampling method; (3) based on this method the distributed parallel computing can be used and we calculate the subsampling probabilities on each subset independently; (4) one by-product of this method is to make statistical inference using bootstrap subsampling, where the advantage about computing time is more obvious. Besides, we extend this subsampling method to the scenario where the response is discrete or categorical and the predictors are functional variables. Moreover, we investigate the asymptotic results of the optimal subsampling estimators for the functional linear model and functional generalized linear model, which is also one of the contributions of our paper. In addition, an R package has been developed for implementing the proposed methods.

The rest of this article is organized as follows. In Section 2, we briefly introduce the functional linear regression and give the estimation and asymptotic properties of the estimators based on the full data. Section 3 derives the optimal subsampling strategy and the optimal subsampling algorithm based on the functional L-optimality criteria for the estimator of the coefficient function. The asymptotic behaviours for the optimal subsampling estimator are also investigated in this section. In Section 4, we extend the optimal subsampling method to the functional generalized linear model. The evaluation of the numerical performance of our proposed estimator via simulation studies is presented

in Section 5. We also illustrate our method by the analysis of two real data sets in Section 6. Some conclusions and discussions are provided in Section 7.

2. Preliminary

2.1. Functional Linear Model

In this paper, we consider a scalar-on-function linear regression model:

$$y_i = \alpha + \int_a^b x_i(t)\beta(t)dt + \varepsilon_i, \quad (1)$$

where the functional predictor $x_i(t)$, $i = 1, \dots, n$ is independent realizations of an unknown process $X(t)$ defined on a domain $[a, b]$, α is the intercept, $\beta(t)$ is the slope function, y_i is the continuous scalar response, the noise term ε_i is i.i.d, and ε_i is independent of $x_i(t)$ that is assumed to be uncorrelated with $E(\varepsilon_i|x_i(t)) = 0$ and $\text{Var}(\varepsilon_i|x_i(t)) = \sigma^2$.

Without loss of generality, the model (1) can be written as a centered model without the intercept:

$$y_i^c = \int_a^b x_i^c(t)\beta(t)dt + \varepsilon_i^c, \quad (2)$$

where $y_i^c = y_i - \bar{y}$, $x_i^c(t) = x_i(t) - \bar{x}(t)$ and $\varepsilon_i^c = \varepsilon_i - \bar{\varepsilon}$ are the centered response, pointwise centered predictor curves and centered noise term, respectively. Once we get an estimate $\hat{\beta}(t)$, the intercept can be estimated as

$$\hat{\alpha} = \bar{y} - \int_a^b \bar{x}(t)\hat{\beta}(t)dt.$$

To ease the notation, we drop the superscript c in (2) from now and focus on the estimation of the coefficient function $\beta(t)$ in the following model

$$y_i = \int_a^b x_i(t)\beta(t)dt + \varepsilon_i.$$

2.2. Full Data Estimation of $\beta(t)$

We utilize the B-spline basis functions (de Boor, 1978) to approximate the slope function. For $p \geq 1$, let $\mathcal{S}(p+1; k) = \{s(\cdot) \in \mathcal{C}^{p+1}[a, b] : s \text{ is a degree } p \text{ polynomial on each } [k_j, k_{j+1}]\}$ be the space of polynomial splines of degree p , implying that the order equals $p+1$. On the domain $[a, b]$, we define a knot sequence with K interior knots $a = k_0 < k_1 < \dots < k_K < k_{K+1} = b$. In addition, define the additional knots:

$$k_{-p} = k_{-p+1} = \dots = k_{-1} = k_0, \quad k_{K+1} = k_{K+2} = \dots = k_{K+p+1}.$$

According to the definition of B-spline basis functions, the total number of basis functions with degree p and K interior knots is $K+p+1$. Denote the p th degree B-spline basis for $\mathcal{S}(p+1; k)$ as $\mathbf{N}(t) = (N_{j,p+1}(t) : -p \leq j \leq K)'$ (Schumaker, 1981).

We denote by $s_\beta(t) = \mathbf{N}'(t)\mathbf{c} \in \mathcal{S}(p+1,)$ the best \mathcal{L}_∞ approximation to function $\beta(t)$ (Claeskens et al., 2009) where $\mathbf{N}'(t)$ denotes the transpose of $\mathbf{N}(t)$. And, the corresponding smoothing estimator for $\beta(t)$ is defined as

$$\hat{\beta}(t) = \mathbf{N}'(t)\hat{\mathbf{c}},$$

where $\hat{\mathbf{c}} = (c_{-p}, \dots, c_K)'$ minimizes the penalized least squares

$$L(\mathbf{c}; \lambda, K) = \sum_{i=1}^n (y_i - \int_a^b x_i(t)\mathbf{N}'(t)dt\mathbf{c})^2 + \lambda \int_a^b \left\{ (\mathbf{N}'(t)\mathbf{c})^{(q)} \right\}^2 dt, \quad (3)$$

with the nonnegative tuning parameter λ . In the above criterion, the first term is the ordinary least squares error, while the second term is the roughness penalty that aims to enforce smoothness of $\hat{\beta}(t)$. It is a natural choice to have $q \leq p$.

Let $\mathbf{D}_q = \int_a^b \mathbf{N}^{(q)}(t)\mathbf{N}^{(q)'}(t)dt$, $\mathbf{y} = (y_1, \dots, y_n)'$, $\mathbf{X}(t) = (x_1(t), \dots, x_n(t))'$, and $\mathbf{N} = \int_a^b \mathbf{X}(t)\mathbf{N}'(t)dt = (\mathbf{N}_1, \dots, \mathbf{N}_n)'$, where $N_i = \int_a^b x_i(t)\mathbf{N}(t)dt$, thus the estimators of \mathbf{c} and $\beta(t)$ are given by

$$\hat{\mathbf{c}} = (\mathbf{N}'\mathbf{N} + \lambda\mathbf{D}_q)^{-1}\mathbf{N}'\mathbf{y} \quad \text{and} \quad \hat{\beta}(t) = \mathbf{N}'(t)(\mathbf{N}'\mathbf{N} + \lambda\mathbf{D}_q)^{-1}\mathbf{N}'\mathbf{y}. \quad (4)$$

2.3. Asymptotic Results of $\hat{\beta}(t)$

In this section, we give the asymptotic results of the estimator $\hat{\beta}(t)$ based on the full data, which is useful to derive the asymptotic distribution of the estimators using the subsampling method. Before we introduce some assumptions used in the following theorems, we first introduce some notations for the clear transparency. If $0 < m < \infty$, \mathcal{L}^m is defined as the space of functions $f(t)$ over the interval $[a, b]$ such that $\int_a^b |f(t)|^m dt < \infty$. With this convention, \mathcal{L}^m is treated as a Banach space with the norm $\|f\|_m = (\int_a^b |f(t)|^m dt)^{1/m}$. When $m = 2$, we get the Hilbert space \mathcal{L}^2 with the inner product $\langle f, g \rangle = \int_a^b f(t)g(t)dt$ and the \mathcal{L}_2 norm $\|f\|_2$. And \mathbb{R}^{m^*} for a positive integer m^* is also a Hilbert space, we also use $\langle \mathbf{u}, \mathbf{v} \rangle = \mathbf{u}'\mathbf{v}$ and $\|\mathbf{u}\|_2 = (\mathbf{u}'\mathbf{u})^{1/2}$ to denote the inner product and the norm of vector \mathbf{u} and \mathbf{v} .

ASSUMPTION 1. Let v be a nonnegative integer, and $\kappa \in (0, 1]$ such that $d = v + \kappa \geq p + 1$. We assume the unknown slope function $\beta(\cdot) \in \mathcal{H}^{(d)}([a, b])$, which is the class of function f on $[a, b]$ whose v th derivative exists and satisfies a Lipschitz condition of order κ : $|f^{(v)}(t) - f^{(v)}(s)| \leq C_v |s - t|^\kappa$, for $s, t \in [a, b]$ and some constant $C_v > 0$.

ASSUMPTION 2. For the functional predictor $X(t)$, it holds that $E(\|X\|_4^4) < \infty$. In addition, the error ε_i term satisfies that $E(\varepsilon_i^4) < \infty$.

ASSUMPTION 3. For the roughness penalty, we assume tuning parameter λ satisfies that $\lambda = o(n^{1/2}K^{1/2-2q})$. Besides, we assume $q \leq p$.

ASSUMPTION 4. Let $\delta_j = k_{j+1} - k_j$ and $\delta = \max_{0 \leq j \leq K} (k_{j+1} - k_j)$. There exists a constant $M > 0$, such that

$$\delta / \min_{0 \leq j \leq K} (k_{j+1} - k_j) \leq M, \quad \max_{0 \leq j \leq K-1} |\delta_{j+1} - \delta_j| = o(K^{-1}). \quad (5)$$

ASSUMPTION 5. The number of knots $K = o(\sqrt{n})$ and $K = \omega(n^{1/(2d+1)})$, where $K = \omega(n^{1/(2d+1)})$ means $K/n^{1/(2d+1)} \rightarrow \infty$ as $n \rightarrow \infty$.

REMARK 2.1. Assumption 1 is about the smoothness of the slope function, which has been widely used in the literature of nonparametric estimation (Liu et al., 2013; Kim and Wang, 2020; Yu et al., 2020b). Assumption 2 gives some moment conditions noise term and functional predictor. Let $\mathbf{G}_{k,n} = \mathbf{N}'\mathbf{N}/n$ and $\mathbf{H}_{k,n} = (\mathbf{G}_{k,n} + \lambda/n\mathbf{D}_q)$. Combing $\|\mathbf{D}_q\|_\infty = O(K^{2q-1})$ with Assumption 3, we can get $\|\lambda\mathbf{D}_q\|_\infty = o(n^{1/2}K^{-1/2})$. Thus, we can get $\|\mathbf{H}_{k,n}\|_\infty = O(1/K)$. Note that (5) in Assumption 4 implies that $\delta \sim K^{-1}$, i.e., δ and K^{-1} are rate-wise equivalent.

THEOREM 1. For any given $t \in [a, b]$, (i) under Assumptions 1-4, we can get

$$\begin{aligned} E\{\hat{\beta}(t) - \beta(t)|X(t)\} &= b_a(t) + b_\lambda(t) + o(K^{-d}) + o(\lambda n^{-1}K^{2q}), \\ \text{Var}\{\hat{\beta}(t)|X(t)\} &= \frac{\sigma^2}{n} \mathbf{N}'(t) \mathbf{H}_{k,n}^{-1} \mathbf{G}_{k,n} \mathbf{H}_{k,n}^{-1} \mathbf{N}(t). \end{aligned}$$

The spline approximation bias is $b_a(t) = -\frac{\beta^d \delta_j^d}{d!} B_d(\frac{t-t_j}{\delta_j}) = O(K^{-d})$, where $B_d(\cdot)$ is the d th Bernoulli polynomial. The shrinkage bias is defined as $b_\lambda = \frac{\lambda}{n} \mathbf{N}'(t) \mathbf{H}_{k,n}^{-1} \mathbf{D}_q \mathbf{c} = O(\lambda K^{2q}/n)$. And, the order of the conditional variance is $\text{Var}\{\hat{\beta}(t)|X(t)\} = O(K/n)$. (ii) Under Assumptions 1-5, as $n \rightarrow \infty$, we have

$$\sqrt{\text{Var}^{-1}\{\hat{\beta}(t)|X(t)\}}(\hat{\beta}(t) - \beta(t)) \xrightarrow{D} N(0, 1).$$

REMARK 2.2. From Assumption 3, we can get $b_\lambda = o(\sqrt{K/n})$, so the shrinkage bias is negligible. And to make the approximation bias negligible, the Assumption 5 ensures that the order of K is n^ν , where $\nu \geq 1/(2d+1)$.

3. Subsampling based estimation

3.1. Subsampling based estimator

Denotes $\mathcal{F}_n = \{(x_i(t), y_i), i = 1, \dots, n; t \in [a, b]\}$ be the full data. Let η_i be the indicator variable that signifies whether $(x_i(t), y_i; t \in [a, b])$ is included in the subdata, that is

$$\eta_i = \begin{cases} 1 & , (x_i(t), y_i; t \in [a, b]) \text{ is included,} \\ 0 & , \text{ otherwise.} \end{cases}$$

and $\eta_i \sim \text{Bernoulli}(p_i)$ with $\sum_{i=1}^n p_i = 1$. Thus, the subsample estimator, denoted as $\tilde{\mathbf{c}}$ is the minimizer of

$$L^*(\mathbf{c}; \lambda, K) = \sum_{i=1}^n \frac{R_i}{L p_i} (y_i - \int_a^b x_i(t) \mathbf{N}(t)' dt \mathbf{c})^2 + \lambda \int_a^b \left\{ (\mathbf{N}(t)' \mathbf{c})^{(q)} \right\}^2 dt, \quad (6)$$

where $R_i = \sum_{l=1}^L \eta_{il}$ denotes the total number of times that i -th observation is selected in to the sample out of the L sampling steps and $R_i \sim B(L, p_i)$. And, we weight the objective function based on the sampling probabilities p_i .

To establish the asymptotic result of the subsample estimator, we need the following Assumption 6. As mentioned in Ai et al. (2021b), Assumption 6 restricts the weights in the estimation equation (6) and ensures the order of the extremely small subsampling probabilities. Besides, this assumption gives the order of the subsampling size L .

ASSUMPTION 6. We assume $\max_{1 \leq i \leq n} (np_i)^{-1} = o_p(\sqrt{L})$ and $L = o(K^2)$.

The following theorem presents the asymptotic normality of the subsample estimator.

THEOREM 2. Under Assumptions 1-6, for any given t , as $L, n \rightarrow \infty$, we have

$$\left\{ \mathbf{N}(t)' \mathbf{H}_{k,n}^{-1} \mathbf{W}_p \mathbf{H}_{k,n}^{-1} \mathbf{N}(t) \right\}^{-1/2} \sqrt{L}(\tilde{\beta}(t) - \beta(t)) \rightarrow N(0, 1).$$

where $\tilde{\beta}(t) = \mathbf{N}(t)' \tilde{\mathbf{c}}$ and

$$\mathbf{W}_p = \frac{1}{n^2} \sum_{i=1}^n \frac{E\{(y_i - \mathbf{N}_i' \mathbf{c})^2\} \mathbf{N}_i \mathbf{N}_i'}{p_i}. \quad (7)$$

REMARK 3.1. In (7), the term $E\{(y_i - \mathbf{N}_i' \mathbf{c})^2\} = \sigma^2 + (\langle x_i, \beta \rangle - \mathbf{N}_i' \mathbf{c})^2$, where σ^2 , $\beta(t)$ and \mathbf{c} are all unknown, so the optimal subsampling probabilities is not directly implementable based the asymptotic variance of $\tilde{\beta}(t)$. To practically implement the optimal subsampling probabilities, we establish the asymptotically normality of $\tilde{\beta}(t) - \hat{\beta}(t)$.

THEOREM 3. Under Assumptions 1-6, for any given t , as $L, n \rightarrow \infty$, conditional on \mathcal{F}_n in probability,

$$\left\{ \mathbf{N}(t)' \mathbf{H}_{k,n}^{-1} \mathbf{V}_p \mathbf{H}_{k,n}^{-1} \mathbf{N}(t) \right\}^{-1/2} \sqrt{L}(\tilde{\beta}(t) - \hat{\beta}(t)) \rightarrow N(0, 1),$$

in distribution, where

$$\mathbf{V}_p = \frac{1}{n^2} \sum_{i=1}^n \frac{\{y_i - \mathbf{N}_i' \hat{\mathbf{c}}\}^2 \mathbf{N}_i \mathbf{N}_i'}{p_i}.$$

3.2. Optimal subsampling probabilities

From Theorem 1 and 2, we can get under some conditions, $\hat{\beta}(t)$ and $\tilde{\beta}(t)$ are both asymptotically unbiased. We want to find the optimal subsampling probabilities that minimizing the asymptotic integrated mean squared error (IMSE) of β in approximating $\hat{\beta}$, which is equal to the asymptotic integrated variance of it. The IMSE is defined as follows,

$$\text{IMSE}(\tilde{\beta} - \hat{\beta}) = \int_a^b \frac{\mathbf{N}(t)' \mathbf{H}_{k,n}^{-1} \mathbf{V}_p \mathbf{H}_{k,n}^{-1} \mathbf{N}(t)}{L} dt. \quad (8)$$

In (8), $L^{-1} \mathbf{H}_{k,n}^{-1} \mathbf{V}_p \mathbf{H}_{k,n}^{-1}$ is the asymptotic covariance matrix of $\tilde{\mathbf{c}} - \hat{\mathbf{c}}$, where $\mathbf{H}_{k,n}$ is related to the smoothing parameter λ to be chosen. In addition, from (8), we can see that only \mathbf{V}_p depends on the sampling probability p_i and the integral $\int_a^b \mathbf{N}(t)' \mathbf{H}_{k,n}^{-1} \mathbf{V}_p \mathbf{H}_{k,n}^{-1} \mathbf{N}(t) dt <$

$\int_a^b \mathbf{N}(t)' \mathbf{H}_{k,n}^{-1} \mathbf{V}_{p^*} \mathbf{H}_{k,n}^{-1} \mathbf{N}(t) dt$ if and only if $\mathbf{V}_p < \mathbf{V}_{p^*}$. We propose to obtain the optimal subsampling probability by minimizing \mathbf{V}_p . There are several criteria to minimize the matrix, here we choose to minimize the trace of the matrix \mathbf{V}_p . It is obvious that $L^{-1} \mathbf{V}_p$ is the asymptotic covariance matrix of $\mathbf{H}_{k,n}^{-1}(\tilde{\mathbf{c}} - \hat{\mathbf{c}})$, where $\mathbf{H}_{k,n}^{-1}(\tilde{\mathbf{c}} - \hat{\mathbf{c}})$ is a linear transformation of the estimator $\tilde{\mathbf{c}} - \hat{\mathbf{c}}$. Thus, minimizing $\text{tr}(\mathbf{V}_p)$ to obtain the optimal subsampling probability is termed the functional L-optimality criterion, which is the functional version of the L-optimality defined in [Pukelsheim \(2006\)](#) and [Atkinson et al. \(2007\)](#).

THEOREM 4. *If the subsampling probabilities $p_i, i = 1, \dots, n$, are chosen as*

$$p_i^{Lopt} = \frac{|y_i - \mathbf{N}_i' \hat{\mathbf{c}}| \|\mathbf{N}_i\|_2}{\sum_{i=1}^n |y_i - \mathbf{N}_i' \hat{\mathbf{c}}| \|\mathbf{N}_i\|_2}, \quad (9)$$

then $\text{tr}(\mathbf{V}_p)$ attains its minimum, where the superscript “Lopt” indicates that this probability is calculated based on the functional L-optimality criterion.

REMARK 3.2. *In (9), p_i^{Lopt} not only directly depends on covariates but also on the response. For the covariates, the term $\|\mathbf{N}_i\|_2 = \|\int_a^b x_i(t) N(t) dt\|_2$ describes the structure information of the covariates, which is similar to statistical leverage score in linear model. The term $|y_i - \mathbf{N}_i' \hat{\mathbf{c}}|$ represents the effect of the responses and it will improve the robustness of the subsample estimator with larger values of $|y_i - \mathbf{N}_i' \hat{\mathbf{c}}|$ in the subsample data.*

Note that the calculation of $\hat{\mathbf{c}}$ in (9) uses full data and takes $O(n(K+p+1)^2)$, we need to replace $\hat{\mathbf{c}}$ by a pilot estimator, say $\hat{\mathbf{c}}_0$, which can be obtained by a uniform subsample with ample size L_0 . In addition, there are a smoothing parameter λ , the parameters for constructing the B-spline basis functions such as the degree p of the B-spline basis and the number of knots K . In penalized spline method, the choice of K is not crucial ([Cardot et al., 2003](#)), as the roughness of the estimator is controlled by a roughness penalty, rather than the number of knots. Usually, in practice, we choose $p = 3$ and K is chosen to be relatively large so that local features of $\beta(t)$ can be captured. Once K and p are fixed, we can select the smoothing parameter λ by Bayesian information criterion (BIC):

$$\text{BIC}(\lambda) = n \log(\|\mathbf{y} - \mathbf{N} \hat{\mathbf{c}}(\lambda)\|_2^2 / n) + \log(n) \text{df}(\lambda),$$

where $\text{df}(\lambda) = \text{tr}(\mathbf{N}(\mathbf{N}' \mathbf{N} + \lambda \mathbf{D}_q)^{-1} \mathbf{N}')$. However, using full data to select the optimal λ is computationally expensive, we need to select the tuning parameter by BIC under the optimal subsample data. Algorithm 1 describes the subsampling procedure for the functional linear in detail.

Recall Assumption 5, the number of knots is required to satisfy that $K = o(\sqrt{n})$ and $K/n^{1/(2d+1)} \rightarrow \infty$ as $n \rightarrow \infty$. Suppose we let the order of K be $n^{1/(2d)}$ in practice. In Algorithm 1, the used subsample size is $L_0 + L \ll n$ and the computing time of the algorithm is $O(n^{1+1/(2d)} + (L_0 + L)n^{1/d})$. And, if the full data size n is very large, the time complexity $O(n^{1+1/(2d)})$ of this subsampling algorithm is much smaller than the computing time $O(n^{1+1/d})$ based on the full data. Thus, the Algorithm 1 can overcome the challenge from computing time. Algorithm 1 is also naturally suited for distributed storage and processing facilities for parallel computing. We can divide the full data into

Algorithm 1 Algorithm motivated by the functional L-optimality for the functional linear model

- **Step 1:** Given a larger K , we generate $\mathbf{N}_i = \int_a^b x_i(t)N(t)dt$ and the new data is $(\mathbf{N}_i, y_i; i = 1, \dots, n)$.
- **Step 2:** Subsample to draw a subsample of size $L_0 < L$ using the uniform sampling probabilities $p_i^0 = 1/n$, and use it to obtain the pilot estimator $\hat{\mathbf{c}}^0$ with $\lambda = 0$.
- **Step 3:** Using $\hat{\mathbf{c}}^0$, we can get the approxiamte optimal subsampling probabilities $p_i^{\text{Lpot}, \hat{\mathbf{c}}^0}$:

$$p_i^{\text{Lpot}, \hat{\mathbf{c}}^0} = \frac{|y_i - \mathbf{N}_i' \hat{\mathbf{c}}^0| \|\mathbf{N}_i\|_2}{\sum_{i=1}^n |y_i - \mathbf{N}_i' \hat{\mathbf{c}}^0| \|\mathbf{N}_i\|_2}.$$

Using the subsampling probabilities $p_i^{\text{Lpot}, \hat{\mathbf{c}}^0}$ to draw a random subsample with replacement of size L . Denote the subsample as $(\mathbf{N}_i^*, y_i^*; t \in [a, b])$, with associated subsampling probabilities $p_i^{*\text{Lpot}, \hat{\mathbf{c}}^0}$.

- **Step 4:** Given λ , then we can obtain the estimate $\check{\mathbf{c}}_{\text{Lopt}}(\lambda)$ through minimizing

$$L_{\text{Lopt}}^*(\mathbf{c}; \lambda, K) = \sum_{i=1}^L \frac{1}{L p_i^{*\text{Lpot}, \hat{\mathbf{c}}^0}} (y_i^* - \mathbf{N}_i^{*'} \mathbf{c})^2 + \lambda \int_a^b \left\{ (\mathbf{N}(t)' \mathbf{c})^{(q)} \right\}^2 dt,$$

and the BIC can be approximated by

$$\text{BIC}_{\text{Lopt}}(\lambda) = L \log(\|\mathbf{y}^* - \mathbf{N}^* \check{\mathbf{c}}_{\text{Lopt}}(\lambda)\|_2^2 / L) + \log(L) \text{df}(\lambda).$$

The optimal λ is selected to minimize $\text{BIC}_{\text{Lopt}}(\lambda)$. Once we get the optimal λ , we can get the estimator $\check{\beta}_{\text{Lopt}}(t) = \mathbf{N}'(t) \check{\mathbf{c}}_{\text{Lopt}}$.

several subsets, simultaneously compute the \mathbf{N}_i and optimal subsample probabilities $p_i^{\text{Lpot}, \hat{\mathbf{c}}^0}$ on each subset. Combining the optimal subsample probabilities of each subset, we can get the indices of a random subsample in the full data and use these indices to extract the corresponding data on each subset.

REMARK 3.3. *Our proposed method can be extended to the following functional linear model with multiple functional covariates:*

$$y_i = \sum_{m=1}^M \int_a^b x_{im}(t) \beta_m(t) dt + \varepsilon_i = \int_a^b \mathbf{x}_i(t)' \boldsymbol{\beta}(t) dt + \varepsilon_i,$$

where y_i is the scalar response, $\mathbf{x}_i(t) = (x_{i1}(t), \dots, x_{iM}(t))'$ is a functional predictor vector defined on domain $[a, b]$, $\boldsymbol{\beta}(t) = (\beta_1(t), \dots, \beta_M(t))'$ and ε_i is the noise. And, the smoothing estimator for $\beta_m(t)$ is defined as

$$\hat{\beta}_m(t) = \mathbf{N}'(t) \hat{\mathbf{c}}_m,$$

where $\hat{\mathbf{c}} = (\hat{\mathbf{c}}_1', \dots, \hat{\mathbf{c}}_M')'$ minimizes the penalized least squares

$$L(\mathbf{c}; \lambda, K) = \sum_{i=1}^n (y_i - \sum_{m=1}^M \int_a^b x_{im}(t) \mathbf{N}'(t) dt \mathbf{c}_m)^2 + \sum_{m=1}^M \lambda_m \int_a^b \left\{ (\mathbf{N}'(t) \mathbf{c}_m)^{(q)} \right\}^2 dt.$$

Let $\mathbf{X}_m(t) = (x_{1m}(t), \dots, x_{nm}(t))'$, for each predictor $x_m(t)$, $m = 1, \dots, M$, we compute a matrix $\mathbf{N}_m = \int_a^b \mathbf{X}_m(t) \mathbf{N}'(t) dt$. Denote $\mathbf{N} = (\mathbf{N}_1, \dots, \mathbf{N}_M)$ be the column catenation of $\mathbf{N}_1, \dots, \mathbf{N}_M$ and corresponding set $\mathbf{D} = \text{diag}(\mathbf{D}_1, \dots, \mathbf{D}_M)$, where \mathbf{D} is the matrix with M blocks \mathbf{D}_q in its main diagonal and zeros elsewhere. After replacing \mathbf{N} and \mathbf{D}_q by new defined \mathbf{N} and \mathbf{D} , respectively, the estimations and algorithms described in Section 2 and Section 3 can be carried out to estimate $\beta_1(t), \dots, \beta_M(t)$ simultaneously. It is worth mentioned that we can simultaneously compute all matrix $\mathbf{N}_1, \dots, \mathbf{N}_M$.

3.3. Asymptotic results of $\check{\beta}_{\text{Lopt}}(t)$

Next theorem shows the asymptotic property of the estimator $\check{\beta}_{\text{Lopt}}(t)$ obtained from Algorithm 1.

THEOREM 5. *If Assumptions 1-6 hold, for any given t , as $L_0 \rightarrow \infty$, $L \rightarrow \infty$ and $n \rightarrow \infty$, conditionally on \mathcal{F}_n in probability,*

$$\left\{ \mathbf{N}(t)' \mathbf{H}_{k,n}^{-1} \mathbf{V}_{\text{Lopt}} \mathbf{H}_{k,n}^{-1} \mathbf{N}(t) \right\}^{-1/2} \sqrt{L} (\check{\beta}_{\text{Lopt}}(t) - \hat{\beta}(t)) \rightarrow N(0, 1),$$

in distribution, where \mathbf{V}_{Lopt} has the minimum trace, and it has the explicit expression

$$\mathbf{V}_{\text{Lopt}} = \frac{1}{n} \sum_{i=1}^n \frac{|y_i - \mathbf{N}_i' \hat{\mathbf{c}}| \mathbf{N}_i \mathbf{N}_i'}{\|\mathbf{N}_1\|_2} \times \frac{1}{n} \sum_{i=1}^n |y_i - \mathbf{N}_i' \hat{\mathbf{c}}| \|\mathbf{N}_1\|_2.$$

4. Extension to functional generalized linear model

In most applications that the response is discrete, the functional linear model may not be sufficient to fit the data. For this scenario, it is intuitive to extend the estimation method in generalized linear model to the model with a discrete scalar response variable and functional predictors. To describe the relationship between the functional predictors and the scalar response from an exponential family distribution (e.g. Binomial distribution and Poisson distribution), we consider a functional generalized linear model, namely, FGLM. James (2002) extends generalized linear models to the model with some functional predictors. And Müller and Stadtmüller (2005) approximates the functional predictor with a truncated Karhunen-Loève expansion and gets the estimators through maximizing a functional quasi-likelihood. Cardot and Sarda (2005), Yao et al. (2005), Crainiceanu et al. (2009), Li et al. (2010), McLean et al. (2014) and Li and Zhu (2020) also study the FGLM and extend the FGLM to semi-parametric FGLM. The basic FGLM is:

$$E(Y|X) = \psi \left(\alpha + \int_a^b Z(t)\beta(t)dt \right),$$

where α is the intercept, $\psi(\cdot)$ is a twice continuously differentiable function and the function $\psi^{-1}(\cdot)$ is called the link function. For example, in the case of logistic functional regression, $\psi(\cdot) = \exp(\cdot)/(1 + \exp(\cdot))$.

4.1. Full data estimation

The intercept α can be represented by the single basis function $1(t)$ as follows: $\alpha = 1(t)\alpha = \int_a^b 1(t)/(b-a)dt\alpha$, where the value of the constant basis $1(t)$ is one everywhere. Denote $\mathbf{Z}(t) = (1(t)/(b-a), Z(t))'$ and $\boldsymbol{\beta}(t) = (\alpha, \beta(t))'$, thus, $\alpha + \int_a^b Z(t)\beta(t)dt = \int_a^b \mathbf{Z}'(t)\boldsymbol{\beta}(t)dt$. Suppose the data $(y_i, \mathbf{z}_i(t)), i = 1, \dots, n$ are i.i.d. copies of $(Y, \mathbf{Z}(t))$. In this section, we replace $\mathbf{N}(t) = \text{diag}(1(t), \mathbf{N}(t))$ and $\mathbf{D}_q = \text{diag}(0, \mathbf{D}_q)$, respectively. Then rewrite \mathbf{N} and \mathbf{N}_i as $\mathbf{N} = \int_a^b \mathbf{X}(t)\mathbf{N}'(t)dt$ and $\mathbf{N}_i = \int_a^b \mathbf{N}(t)\mathbf{z}_i(t)dt$, where $\mathbf{X}(t) = (\mathbf{z}_1(t), \dots, \mathbf{z}_n(t))'$.

Combining the maximum quasi-likelihood estimator in generalized linear model (Chen et al., 1999; Müller and Stadtmüller, 2005) and the penalized B-spline, we can get the penalized quasi-likelihood estimator $\hat{\boldsymbol{\beta}}_{\text{PQL}}(t) = \mathbf{N}'(t)\hat{\mathbf{c}}_{\text{PQL}}$, where $\hat{\mathbf{c}}_{\text{PQL}}$ can be obtained by solving the following equation :

$$Q_{\text{PQL}}(\mathbf{c}) = \sum_{i=1}^n \{y_i - \psi(\mathbf{N}_i'\mathbf{c})\}\mathbf{N}_i - \lambda \mathbf{D}_q \mathbf{c} = 0. \quad (10)$$

ASSUMPTION 7. Let $\dot{Q}_{\text{PQL}}(\gamma, y)$ be the first order derivative of $Q_{\text{PQL}}(\gamma, y)$ with respect to γ . The function $\dot{Q}_{\text{PQL}}(\gamma, y) < 0$ for $\eta \in \mathbb{R}$ and y in the range of the response variable. The functions $\psi(\cdot)$, the first order derivative of $\psi(\cdot)$ are continuous, and there exist positive constants c_Q and C_Q such that $c_Q \leq \dot{Q}_{\text{PQL}}(\gamma, y) \leq C_Q$. In addition, $E(\|\mathbf{Z}\|_4^4) < \infty$ and for each \mathbf{z} , $\text{Var}(Y|\mathbf{Z} = \mathbf{z})$ and $\psi^{-1}(\int_a^b \mathbf{z}'(t)\boldsymbol{\beta}(t)dt)$ are nonzero.

The above assumption is a common assumptions used under the quasi likelihood frame work (Carroll et al., 1997; Wang et al., 2011; Liu et al., 2013; Wang et al., 2018b; Kim and Wang, 2020; Yu et al., 2020b). And $\dot{Q}_{PQL}(\eta, y) < 0$ ensures the uniqueness of the solution (10).

Denote $\Psi = \text{Diag}(\dot{\psi}(N_1'c), \dots, \dot{\psi}(N_n'c))$, $G_{k,n}^\psi = \frac{1}{n}N'\Psi N$ and $H_{k,n}^\psi = G_{k,n}^\psi + \lambda D_q$, where $\dot{\psi}(\cdot)$ is the first order derivative of $\psi(\cdot)$. The asymptotic property of $\hat{\beta}_{PQL}(t)$ is given in the next theorem.

THEOREM 6. *Under Assumptions 1-5 and 7, for any given t , as $n \rightarrow \infty$, we have*

$$\sqrt{\text{Cov}^{-1}\{\hat{\beta}_{PQL}(t)|X(t)\}}(\hat{\beta}_{PQL}(t) - \beta(t)) \xrightarrow{D} N(\mathbf{0}_2, \mathbf{I}_2),$$

where $\mathbf{0}_n$ is an $n \times 1$ vector with 0s and

$$\text{Cov}\{\hat{\beta}_{PQL}(t)|X(t)\} = \frac{\sigma^2}{n}N'(t)H_{k,n}^{\psi,-1}G_{k,n}H_{k,n}^{\psi,-1}N(t).$$

4.2. Subsampling based estimation

The subsample penalized quasi-likelihood estimator, denoted as $\tilde{\beta}_{PQL}(t)$ is given by

$$\tilde{\beta}_{PQL}(t) = N'(t)\tilde{c}_{PQL},$$

where \tilde{c}_{PQL} can be obtained through the equation

$$Q_{PQL}^*(c) := \sum_{i=1}^n \frac{R_i}{Lp_i} \{y_i - \psi(N_i'c)\}N_i - \lambda D_q c = 0.$$

THEOREM 7. *Under Assumptions 1-7, for any given t , as $L, n \rightarrow \infty$, we have*

$$\left\{N(t)'H_{k,n}^{\psi,-1}W_p^\psi H_{k,n}^{\psi,-1}N(t)\right\}^{-1/2} \sqrt{L}(\tilde{\beta}_{PQL}(t) - \beta(t)) \rightarrow N(\mathbf{0}_2, \mathbf{I}_2).$$

where

$$W_p^\psi = \frac{1}{n^2} \sum_{i=1}^n \frac{E\left\{(y_i - \psi(N_i'c))^2\right\}N_i N_i'}{p_i}. \quad (11)$$

REMARK 4.1. In (11), the term $E\left\{(y_i - \psi(N_i'c))^2\right\}$ is unknown, so the optimal subsampling probabilities is not directly implementable based the asymptotic variance of $\tilde{\beta}_{PQL}(t)$. Similar with Section 3.1, we establish the asymptotically normality of estimator $\tilde{\beta}_{PQL}(t)$ in approximating the full data estimator $\hat{\beta}_{PQL}(t)$ to obtain the optimal subsampling probabilities.

THEOREM 8. *Under Assumptions 1-7, for any given t , as $L, n \rightarrow \infty$, conditionally on \mathcal{F}_n in probability,*

$$\left\{N(t)'H_{k,n}^{\psi,-1}V_p^\psi H_{k,n}^{\psi,-1}N(t)\right\}^{-1/2} \sqrt{L}(\tilde{\beta}_{PQL}(t) - \hat{\beta}_{PQL}(t)) \rightarrow N(\mathbf{0}_2, \mathbf{I}_2),$$

where

$$V_p^\psi = \frac{1}{n^2} \sum_{i=1}^n \frac{\{y_i - \psi(N_i'\hat{c}_{PQL})\}^2 N_i N_i'}{p_i}.$$

4.3. Optimal subsampling probabilities

Under some conditions, $\hat{\beta}_{PQL}(t)$ and $\tilde{\beta}_{PQL}(t)$ are both asymptotically unbiased. We want to find the optimal subsampling probabilities that minimizing IMSE of $\tilde{\beta}_{PQL}$ in approximating $\hat{\beta}_{PQL}$, where the IMSE is defined as follows,

$$\text{IMSE}(\tilde{\beta}_{PQL} - \hat{\beta}_{PQL}) = \int_a^b \frac{\mathbf{N}(t)' \mathbf{H}_{k,n}^{\psi,-1} \mathbf{V}_p^\psi \mathbf{H}_{k,n}^{\psi,-1} \mathbf{N}(t)}{L}. \quad (12)$$

From (12), it is clear that only \mathbf{V}_p^ψ depends on p_i 's, therefore, similar to the subsampling method in the functional linear, we use the functional L-optimality criterion that is minimizing the $\text{tr}(\mathbf{V}_p^\psi)$ to get the optimal subsampling probabilities.

THEOREM 9. *If the subsampling probabilities $p_i, i = 1, \dots, n$, are chosen as*

$$p_{PQL,i}^{\text{Lopt}} = \frac{|y_i - \psi(\mathbf{N}_i' \hat{\mathbf{c}}_{PQL})| \|\mathbf{N}_i\|_2}{\sum_{i=1}^n |y_i - \psi(\mathbf{N}_i' \hat{\mathbf{c}}_{PQL})| \|\mathbf{N}_i\|_2}, \quad (13)$$

then $\text{tr}(\mathbf{V}_p^\psi)$ attains its minimum.

REMARK 4.2. *Analogous to the optimal subsampling probabilities (9) for the functional linear model, the subsampling probabilities (13) are related with the covariates and response. Suppose the response $y_i \in \{0, 1\}, i = 1, \dots, n$, we study the effect of the response on the subsampling probabilities. For these individuals with response $y_i = 1$, a smaller estimated probability $\psi(\mathbf{N}_i' \hat{\mathbf{c}}_{PQL})$ using full data results in a larger subsampling probability $p_{PQL,i}^{\text{Lopt}}$. On the contrary, for these samples with $y_i = 0$, the subsampling probability $p_{PQL,i}^{\text{Lopt}}$ increases as the estimated probability $\psi(\mathbf{N}_i' \hat{\mathbf{c}}_{PQL})$ increases. In summary, this subsampling method is more likely to select those samples that are more easily misclassified, which means this method improves the robustness of the subsample estimator.*

Akin to the subsampling steps in the functional linear, we give the practical subsampling procedure for FGLM in Algorithm 2.

As in functional linear model, we suppose the order of K used in the estimation of functional generalized linear model is $n^{1/(2d)}$. In Algorithm 2, we need to use an iterative procedure, such as Newton's method, to get the pilot estimator and solve (14). In step 1 & 3, it takes $O(n^{1+1/(2d)})$ computing time to calculate the matrix \mathbf{N} and the subsampling probabilities. To get the pilot estimator $\hat{\mathbf{c}}_{PQL}^0$ in step 2, the computing time is $O(\xi_0 L_0 n^{1/d})$ where ξ_0 is the number of iterations. In step 3, for each iteration, it takes $O(L n^{1/d})$ computing time and the whole procedure requires $O(\xi L n^{1/d})$ with the number of iterations ξ . Thus, when the full data size n is very large, total computing time $O(n^{1+1/(2d)} + \xi_0 L_0 n^{1/d} + \xi L n^{1/d}) \approx O(n^{1+1/(2d)})$ is smaller than the total computing time based on full data $O(n^{1+1/(2d)} + \xi_{full} n^{1+1/d}) \approx O(n^{1+1/d})$.

The asymptotic result of the estimator obtained from Algorithm 2 is presented as follows.

Algorithm 2 Algorithm motivated by the functional L-optimality for the functional generalized linear model

- **Step 1:** Given a larger K , we generate $\mathbf{N}_i = (1, \int_a^b z_i(t)N'(t)dt)'$ and the new data is $(\mathbf{N}_i, y_i; i = 1, \dots, n)$.
- **Step 2:** Subsample to draw a subsample of size $L_0 < L$ using the uniform sampling probabilities $p_i^0 = 1/n$, and use it to obtain the pilot estimator $\hat{\mathbf{c}}_{PQL}^0$ with $\lambda = 0$.
- **Step 3:** Using $\hat{\mathbf{c}}_{PQL}^0$, we can get the approximate optimal subsampling probabilities $p_{PQL,i}^{\text{Lpot}, \hat{\mathbf{c}}^0}$:

$$p_{PQL,i}^{\text{Lpot}, \hat{\mathbf{c}}^0} = \frac{|y_i - \psi(\mathbf{N}_i' \hat{\mathbf{c}}_{PQL}^0)| \|\mathbf{N}_i\|_2}{\sum_{i=1}^n |y_i - \psi(\mathbf{N}_i' \hat{\mathbf{c}}_{PQL}^0)| \|\mathbf{N}_i\|_2},$$

Using the subsampling probabilities $p_{PQL,i}^{\text{Lpot}, \hat{\mathbf{c}}^0}$ to draw a random subsample with replacement of size L . Denote the subsample as (\mathbf{N}_i^*, y_i^*) , with associated subsampling probabilities $p_{PQL,i}^{*\text{Lpot}, \hat{\mathbf{c}}^0}$.

- **Step 4:** Given λ , then we can obtain the estimate $\hat{\mathbf{c}}_{\text{Lopt}}^{\text{PQL}}(\lambda)$ through solving

$$Q_{PQL}^{*\text{Lopt}}(\mathbf{c}) = \sum_{i=1}^L \frac{1}{L p_{PQL,i}^{*\text{Lpot}, \hat{\mathbf{c}}^0}} (y_i^* - \psi(\mathbf{N}_i^{*'} \mathbf{c})) \mathbf{N}_i - \lambda \mathbf{D}_q = 0, \quad (14)$$

and based on the optimal subsample data, we can use BIC to choose the optimal tuning parameter λ . Once we get the optimal λ , we can get the estimator $\hat{\beta}_{PQL}^{\text{Lopt}}(t) = \mathbf{N}'(t) \hat{\mathbf{c}}_{\text{Lopt}}^{\text{PQL}}$.

THEOREM 10. Under Assumptions 1-7, for any given t , as $L_0 \rightarrow \infty$, $L \rightarrow \infty$ and $n \rightarrow \infty$, conditionally on \mathcal{F}_n in probability,

$$\left\{ \mathbf{N}(t)' (\mathbf{H}_{k,n}^\psi)^{-1} \mathbf{V}_{Lopt}^\psi (\mathbf{H}_{k,n}^\psi)^{-1} \mathbf{N}(t) \right\}^{-1/2} \sqrt{L} (\check{\beta}_{PQL}^{Lopt}(t) - \hat{\beta}_{PQL}(t)) \rightarrow \mathbb{N}(\mathbf{0}_2, \mathbf{I}_2),$$

in distribution, where \mathbf{V}_{Lopt}^ψ has the minimum trace, and it has the explicit expression

$$\mathbf{V}_{Lopt}^\psi = \frac{1}{n} \sum_{i=1}^n \frac{|y_i - \psi(\mathbf{N}_i' \hat{\mathbf{c}}_{PQL})| \mathbf{N}_i \mathbf{N}_i'}{\|\mathbf{N}_1\|_2} \times \frac{1}{n} \sum_{i=1}^n |y_i - \psi(\mathbf{N}_i' \hat{\mathbf{c}}_{PQL})| \|\mathbf{N}_1\|_2.$$

5. Simulation Studies

In this section, we conduct three simulation studies to illustrate the good performance of the subsample estimators obtained from Algorithm 1 and Algorithm 2.

5.1. Simulation I

To investigate the numerical performance of the subsample estimator based on the functional L-optimality-motivated algorithm described in Algorithm 1, we consider synthetic data of 500 runs generated from the following functional linear model

$$y_i = \int_0^1 x_i(t) \beta(t) dt + \varepsilon_i, \quad i = 1, \dots, n,$$

where $\varepsilon_i \stackrel{iid}{\sim} N(0, \sigma^2)$, $\beta(t) = \exp(-32(t - 0.5)^2) + 2t - 1$ and $\sigma^2 = 0.1$. The predictor functions $x_i(t)$ are generated by $x_i(t) = \sum a_{ij} B_j(t)$, where $B_j(t)$ are cubic B-spline basis functions defined on 66 equally spaced knots over $[0, 1]$, and we consider the following three different scenarios to generate the coefficients a_{ij} ,

- **Scenario I.** The coefficient a_{ij} are i.i.d from the standard normal distribution, namely, $a_{ij} \stackrel{iid}{\sim} N(0, 1)$.
- **Scenario II.** We generate the coefficient a_{ij} from t distribution with 3 degree of freedom and the variance is 1, namely, $a_{ij} \stackrel{iid}{\sim} t_3(0, 1)$.
- **Scenario III.** We generate the coefficient a_{ij} from t distribution with 2 degree of freedom and the variance is 1, namely, $a_{ij} \stackrel{iid}{\sim} t_2(0, 1)$.

When the sample size $n = 10^5$, a random subset of 10 curves for predictor functions $x_i(t)$ under three scenarios are presented in Fig. 1. From Fig. 1, we can see that the variation among the predictor functions $x_i(t)$ is the smallest when a_{ij} is generated from Scenario I, and the variation is the largest when a_{ij} is generated from Scenario III, which means that the data generated under Scenario I is more uniform.

In the following, we want to compare two different approaches: the functional L-optimality-motivated algorithm described in Algorithm 1 (Lopt, black line) and the uniform subsampling approach (Unif, red line). For the fairness of comparison, we use

the same K and λ in the two approaches when the full data sizes are the same. And the IMSEs of $\tilde{\beta}$ from 500 replications is defined as follows:

$$\text{IMSE} = \frac{1}{500} \sum_{s=1}^{500} \int (\tilde{\beta}^{(s)}(t) - \beta(t))^2 dt.$$

For full data size $n = 10^5, 10^6, 5 \times 10^6$, we present the IMSE of the resultant estimator under three scenarios, respectively. Fig. 2 (a)-(c) show the mean of IMSE corresponding to the subsample sizes of 600, 800, 1000, 1200, 1400 and 1600 when the full data size $n = 10^5$. When the full data size $n = 10^6$, we choose the subsample size $L = 1000, 2000, 3000, 4000, 5000, 6000$ and the result is presented in Fig. 2 (d)-(f). See Fig. 2 (g)-(i) for the IMSE of the resultant estimator with $n = 5 \times 10^6$ and subsample size $L = 5000, 6000, 7000, 8000, 9000, 10000$.

From Fig. 2, it is clear that for three cases, $p^{\text{Lopt}, \hat{c}^0}$ (Lopt) always results in smaller IMSE than the Unif method, which is consistent with the theoretical results that aim to minimize the IMSE of the resultant estimator. We can also see that the advantage of Lopt method is more significant when the tail of the coefficient a_{ij} is heavier. And, these figures show that the IMSE from both methods decreases as the subsample size L increases when the full data size n is fixed, namely, the IMSE decreases as the ratio L/n increases.

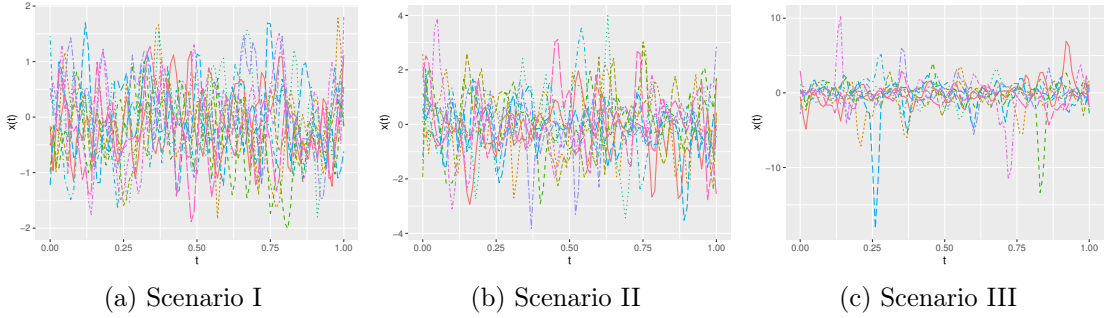


Fig. 1: A random subset of 10 curves of $x_i(t)$ under three scenarios when the full sample size is $n = 10^5$.

To evaluate the computational efficiency of the subsampling strategies, we record the CPU times (in seconds) of the two subsampling strategies and full data strategy. In this paper, we use the R programming language to implement each method and all computations are carried on a desktop running Windows 7 with an Intel I5 processor and 8GB memory.

Table 1 gives the results for different combinations of the full data size n and the subsample size L under Scenario I. The results under the other two scenarios are similar and thus omitted. From this table, it is clear that the Lopt method outperforms the full data method. Besides, the difference between Lopt method and Unif is very small, so the Lopt is comparable to the Unif method. Moreover, when the number of knots $K = 500$ and the full size $n = 5 \times 10^6$, the memory that the matrix \mathbf{N} needs is about 19.6G, which

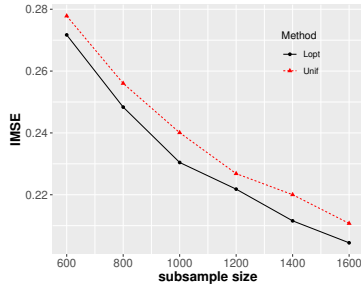
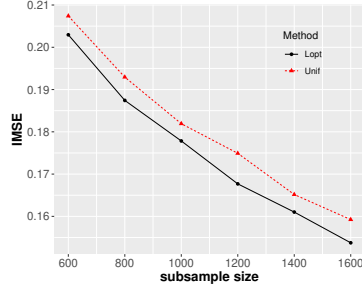
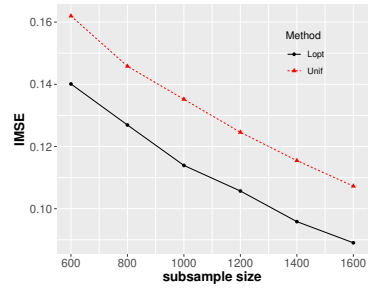
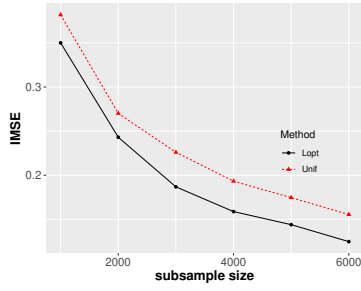
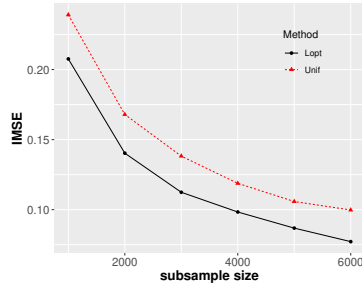
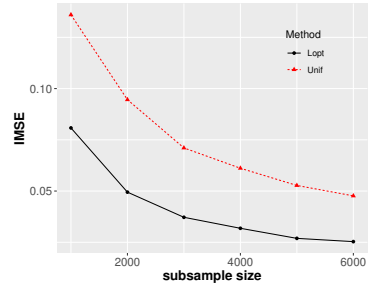
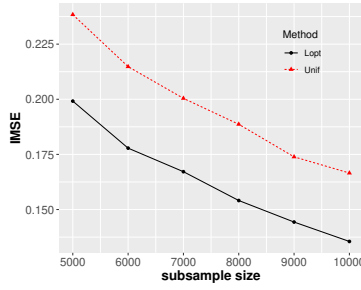
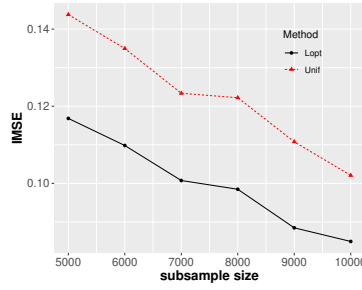
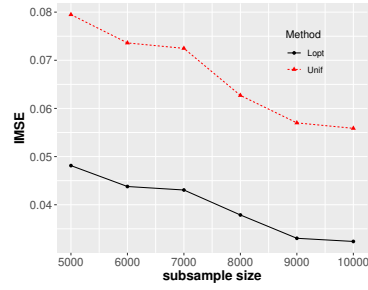
(a) Scenario I, $n = 10^5$ (b) Scenario II, $n = 10^5$ (c) Scenario III, $n = 10^5$ (d) Scenario I, $n = 10^6$ (e) Scenario II, $n = 10^6$ (f) Scenario III, $n = 10^6$ (g) Scenario I, $n = 5 \times 10^6$ (h) Scenario II, $n = 5 \times 10^6$ (i) Scenario III, $n = 5 \times 10^6$

Fig. 2: IMSEs for different subsample sizes L and full data size n in the functional linear model under three scenarios.

exceeds the maximum memory of a general computer with 16G, so the full data method is not feasible. In this case, for Lopt method and Unif method, we can parallel computing to calculate \mathbf{N} , $p^{\text{Lopt}, \hat{\mathbf{c}}^0}$ and then using the optimal subsampling data to estimate $\beta(t)$.

Table 1: CPU times for different methods in the functional linear model with different full data sizes and the number of knots $K = 500$ when the tuning parameter λ is fixed.

The full data size $n = 10^5$.						
Method	L					
	1000	2000	3000	4000	5000	6000
Lopt	0.449	0.517	0.585	0.610	0.626	0.675
Unif	0.149	0.191	0.221	0.257	0.293	0.347
Full	28.953					
The full data size $n = 10^6$.						
Method	L					
	1000	2000	3000	4000	5000	6000
Lopt	5.896	6.323	6.782	8.244	9.026	11.982
Unif	1.423	1.995	2.758	3.326	4.852	7.652
Full	135.759					
The full data size $n = 5 \times 10^6$.						
Method	L					
	5000	6000	7000	8000	9000	10000
Lopt	18.866	22.206	26.910	30.141	34.983	51.894
Unif	5.368	9.557	13.449	16.651	24.486	38.340
Full	NA					

5.2. Simulation II

In this section, we take functional logistic regression as an example to evaluate the finite sample performance of the proposed method, the functional L-optimality-motivated algorithm described in Algorithm 3. We set $\beta(t) = \sin(0.5\pi t)$ and the designs of the functional predictors $x_i(t)$ are the same as in Simulation I, except that we consider the following four different scenarios to generate the coefficients a_{ij} ,

- **Scenario I.** The coefficient a_{ij} are i.i.d from $\sim N(0, 15)$. From Fig. 3 (a), we can see that in the generated data set under this scenario, the distribution of the probability $p(x_i)$ is symmetric about 0.5 and the number of 1's and the number of 0's in the responses are roughly equal.
- **Scenario II.** We generate the coefficient a_{ij} from t distribution with 2 degree of freedom and zero mean, namely, $a_{ij} \stackrel{iid}{\sim} t_2$. For this scenario, Fig. 3 (b) shows that the probability $p(x_i)$ is symmetric about 0.5 and is less uniform than these $p(x_i)$ of Scenario I. Similar with the Scenario I, in the generated data set under this scenario, the number of 1's and the number of 0's in the responses are roughly equal.
- **Scenario III.** Similar with the setting in Wang et al. (2018a), we generate the coefficient a_{ij} from $N(1.5, 15)$. In this scenario, the distribution of probability $p(x_i)$

is skewed left and about 67.09% of responses are 1, which can be seen from Fig. 3 (c). This data set is an imbalanced data.

- **Scenario IV.** We generate the coefficient a_{ij} from $N(-3.0, 15)$. The data set generated under this scenario is an example of rare events data and about 18.87% of responses are 1, which is in accordance the numerical evaluations of rare event data in Wang et al. (2018a). From Fig. 3 (d), we can see that the distribution of probability $p(x_i)$ is skewed right.

The designs of the functional predictors $x_i(t)$ and $\beta(t)$ are the same as in Simulation I. Denote $\psi(\cdot) = \exp(\cdot)/(1 + \exp(\cdot))$ and $p(x_i) = \psi(\int_0^1 x_i(t)\beta(t)dt)$, then we generated responses $y(x) \sim \text{Binomial}(p(x), 1)$ as pseudo-Bernoulli r.v.s with probability $p(x)$.

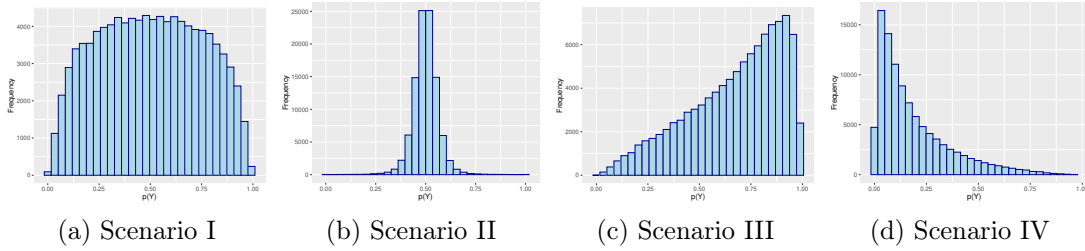


Fig. 3: The histogram of $p(x_i)$ under four scenarios when the full data size is $n = 10^5$.

Fig. 4 (a)-(l) show the mean of IMSE under full data size 10^5 , 10^6 and 5×10^6 , respectively. From these figures, it is obvious that the IMSEs for both methods decrease as the subsample increases, and the Lopt method outperforms the Unif method for all scenarios and full data size. When the full data size is fixed, from the IMSE plots under Scenario I, II and IV, the more imbalanced the data, the greater the advantage of Lopt method over Unif method. When the proportion of 1's in the responses reaches 4.33% ($a_{ij} \stackrel{iid}{\sim} N(-6, 15)$) or even 1.34% ($a_{ij} \stackrel{iid}{\sim} N(-8, 15)$), our method still can outperform the Unif method, which can be seen from Fig. 5. However, it should be pointed that when the data is extremely rare data (e.g. 0.02% of 1's in the responses, that is, $a_{ij} \stackrel{iid}{\sim} N(-15, 15)$), our method does not work well, nor do Unif method and the method using full data. And the simulation results about the extreme data are not presented in this paper. From Fig. 4 (b), Fig. 4 (f) and Fig. 4 (j), we can see that the Lopt method always dominates the Unif method when the generated data set is not uniform.

To show the performance of these two methods on the classification, we present the plots of proportions of correct classifications (PCC) on the responses in Fig. 6, and the PCC is defined as :

$$\text{PCC} = \frac{\#\{y_i = 1 \text{ and } \psi(\mathbf{N}'_i \hat{\mathbf{c}}) > 0.5\} + \#\{y_i = 0 \text{ and } \psi(\mathbf{N}'_i \hat{\mathbf{c}}) \leq 0.5\}}{n}.$$

As shown in these three figures, the Lopt performs better than Unif method in all scenarios. And for Scenario II, although the two methods do not perform well, Lopt is still slightly better than Unif. Under Scenario II, the performance using full data is also not good, which is not presented in these figures.

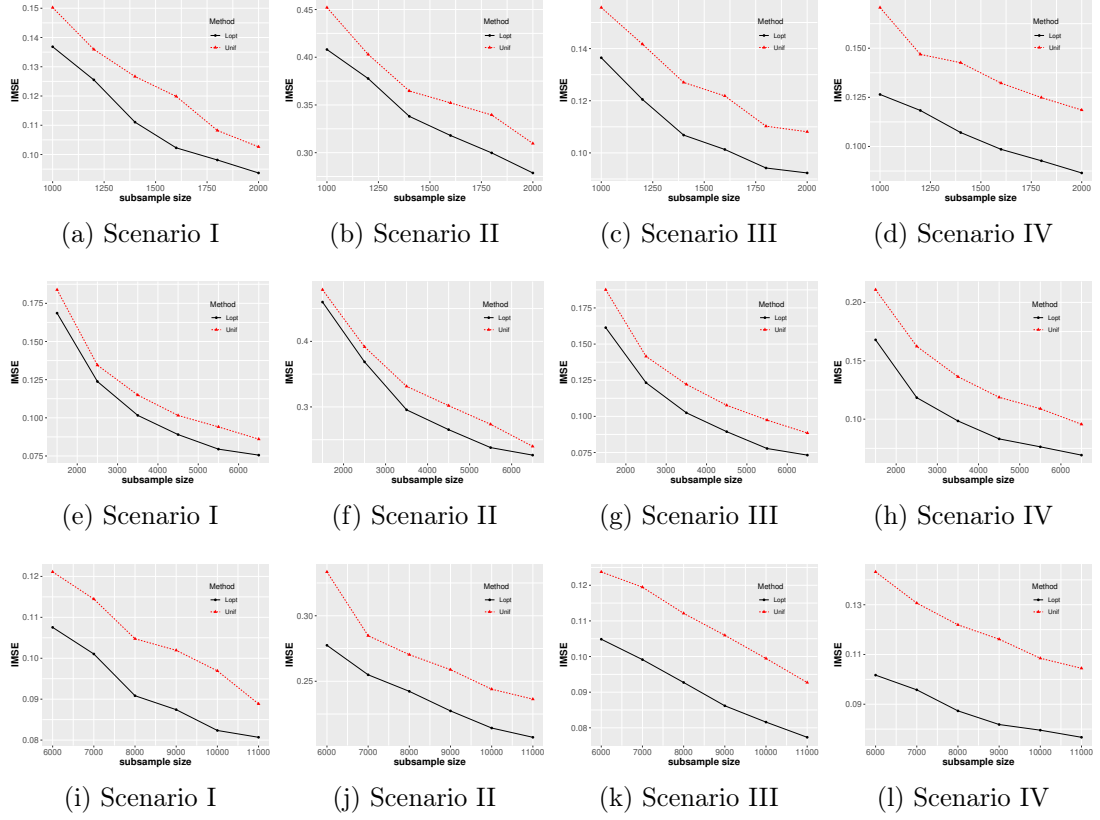


Fig. 4: When the response $y(x) \sim \text{Binomial}(p(x), 1)$, (a)-(d) show the IMSEs for different subsample sizes L and different scenarios under the full data size $n = 10^5$, (e)-(h) show the IMSEs for different subsample sizes L and different scenarios under the full data size $n = 10^6$, (i)-(l) show the IMSEs for different subsample sizes L and different scenarios under the full data size $n = 5 \times 10^6$.

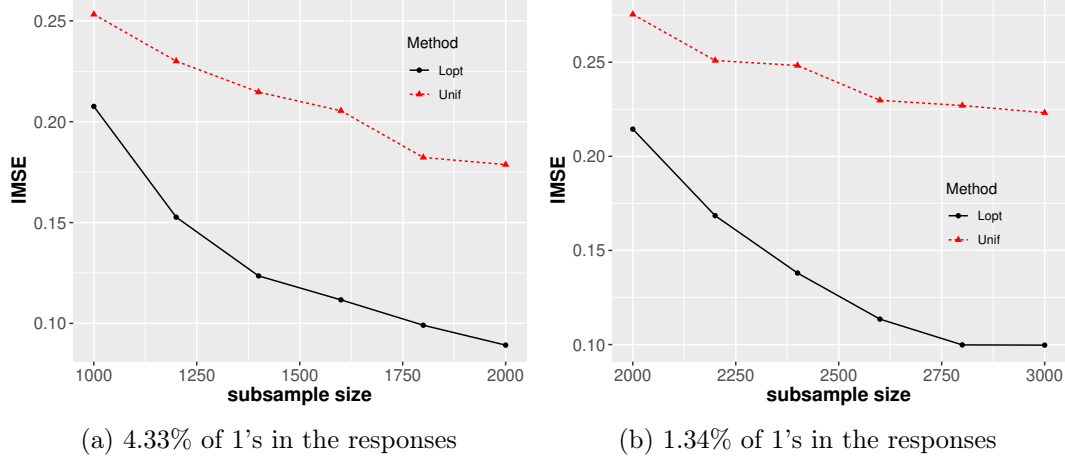


Fig. 5: (a) IMSEs for the rare event data with 4.33% of 1's in the responses when the full data size $n = 10^5$ and subsample size $L = 1000, 1200, 1400, 1600, 1800, 2000$. (b) IMSEs for the rare event data with 1.34% of 1's in the responses when the full data size $n = 10^5$ and subsample size $L = 2000, 2200, 2400, 2600, 2800, 3000$.

As mentioned above, regardless of whether the generated functional covariates are uniform or the responses are imbalanced, our proposed Lopt method is better than the Unif method.

5.3. Simulation III

In this section, we take functional Poisson regression as an example to evaluate the finite sample performance of the proposed subsampling method described in Algorithm 2. We set $\beta(t) = \sin(0.5\pi t)$ and the designs of the functional predictors $x_i(t)$ are the same as in Simulation I, except that we consider the following three different scenarios to generate the coefficients a_{ij} ,

- **Scenario I.** The coefficient a_{ij} are i.i.d from the standard normal distribution, namely, $a_{ij} \stackrel{iid}{\sim} N(0, 1)$. From Fig. 7 (a) and Fig. 7 (d), it is easy to see that the distribution of the expected value $\lambda(x_i)$ ranges from 0.6 to 1.5 and is approximately symmetric about 1. Accordingly, about 70% of responses are equal to 0 or 1.
- **Scenario II.** We generate the coefficient a_{ij} from t distribution with 4 degree of freedom and the variance is 1, namely, $a_{ij} \stackrel{iid}{\sim} t_4(0.5, 1)$. The $\lambda(x_i)$ varies from 0.6 to 1.5 and about 80% of responses lie between 0-2.
- **Scenario III.** We generate the coefficient a_{ij} from the uniform distribution between 0 and 4, namely, $a_{ij} \stackrel{iid}{\sim} U(0, 4)$. The expected value $\lambda(x_i)$ ranges from 2 to 6 and the distribution of responses is more uniform than the above two scenarios, which can be found in Fig. 7 (c) and Fig. 7 (f).

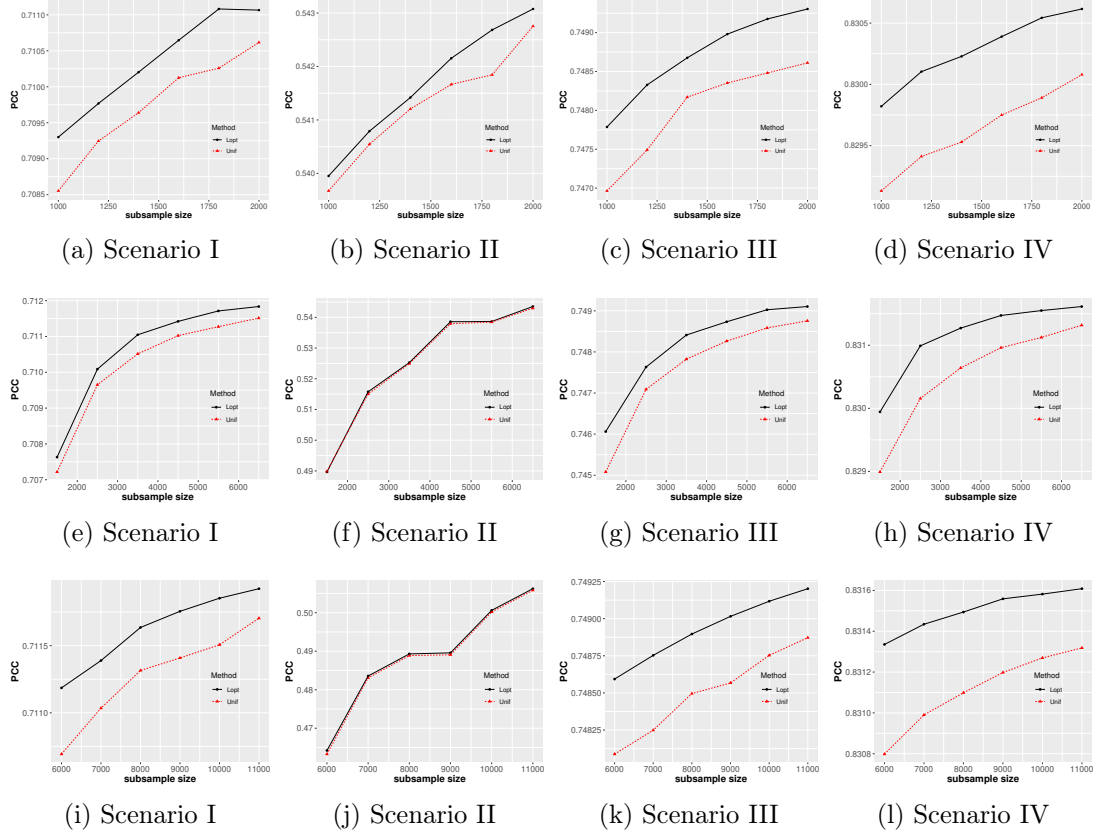


Fig. 6: When the response $y(x) \sim \text{Binomial}(p(x), 1)$, (a)-(d) show the PCCs for different subsample sizes L and different scenarios under the full data size $n = 10^5$, (e)-(h) show the PCCs for different subsample sizes L and different scenarios under the full data size $n = 10^6$, (i)-(l) show the PCCs for different subsample sizes L and different scenarios under the full data size $n = 5 \times 10^6$.

Denote $\psi(\cdot) = \exp(\cdot)$ and $\lambda(x_i) = \psi(\int_0^1 x_i(t)\beta(t)dt)$, then we generated responses $y(x) \sim \text{Poisson}(\lambda(x))$ as pseudo-Poisson r.v.s with mean $\lambda(x)$.

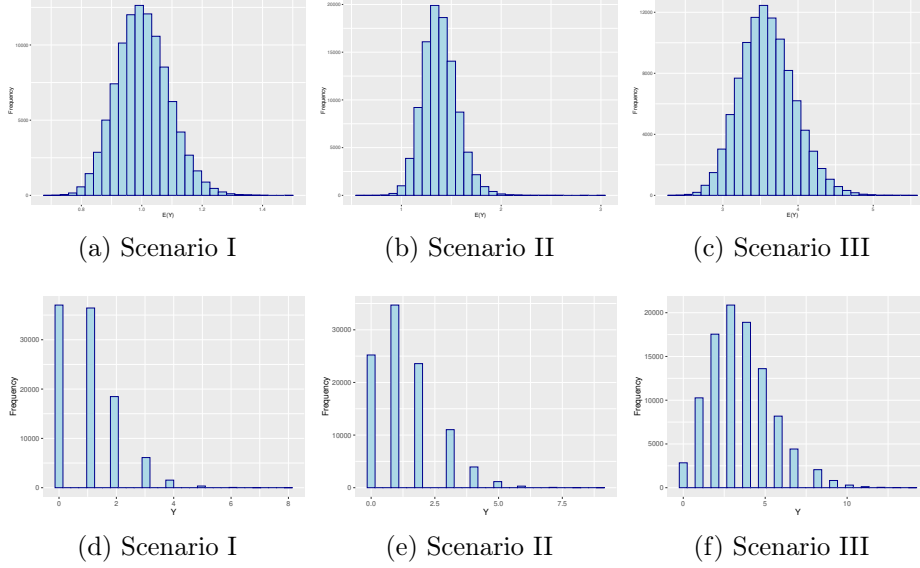


Fig. 7: (a)-(c) show the histogram of $\lambda(x_i)$ and (d)-(f) show the histogram of y_i under three scenarios when the full data size is $n = 10^5$.

Fig. 8 shows the mean of IMSEs for the Lopt and Unif method under different scenarios and full data size. From these figures, it is clear that the Lopt method outperforms Unif method for all scenarios and full data size, which is consistent with the theoretical results that it aims to minimize the IMSE of the resultant estimator in approximating the estimator using full data. Besides, when the full data size is fixed, the IMSEs of both methods become smaller as the subsample size L increases.

6. Application

In this section, we use two real data sets, the global climate data set and the kidney transplant data set, to illustrate the performance of the proposed subsampling algorithm 1 and 2.

6.1. Global climate data

In recent years, climate change has created enormous challenges and costs for societies worldwide. For example, climate change is considered very likely to have contributed to the unprecedented extent and severity of the 2019–20 Australian bushfires. Thus, climate change is a global issue that should be addressed and emphasized.

Rising temperature is the most obvious feature of climate change. According to the Intergovernmental Panel on Climate Change's (IPCC) fifth assessment report (http://www.climatechange2013.org/images/report/WG1AR5_TS_FINAL.pdf), it is extremely

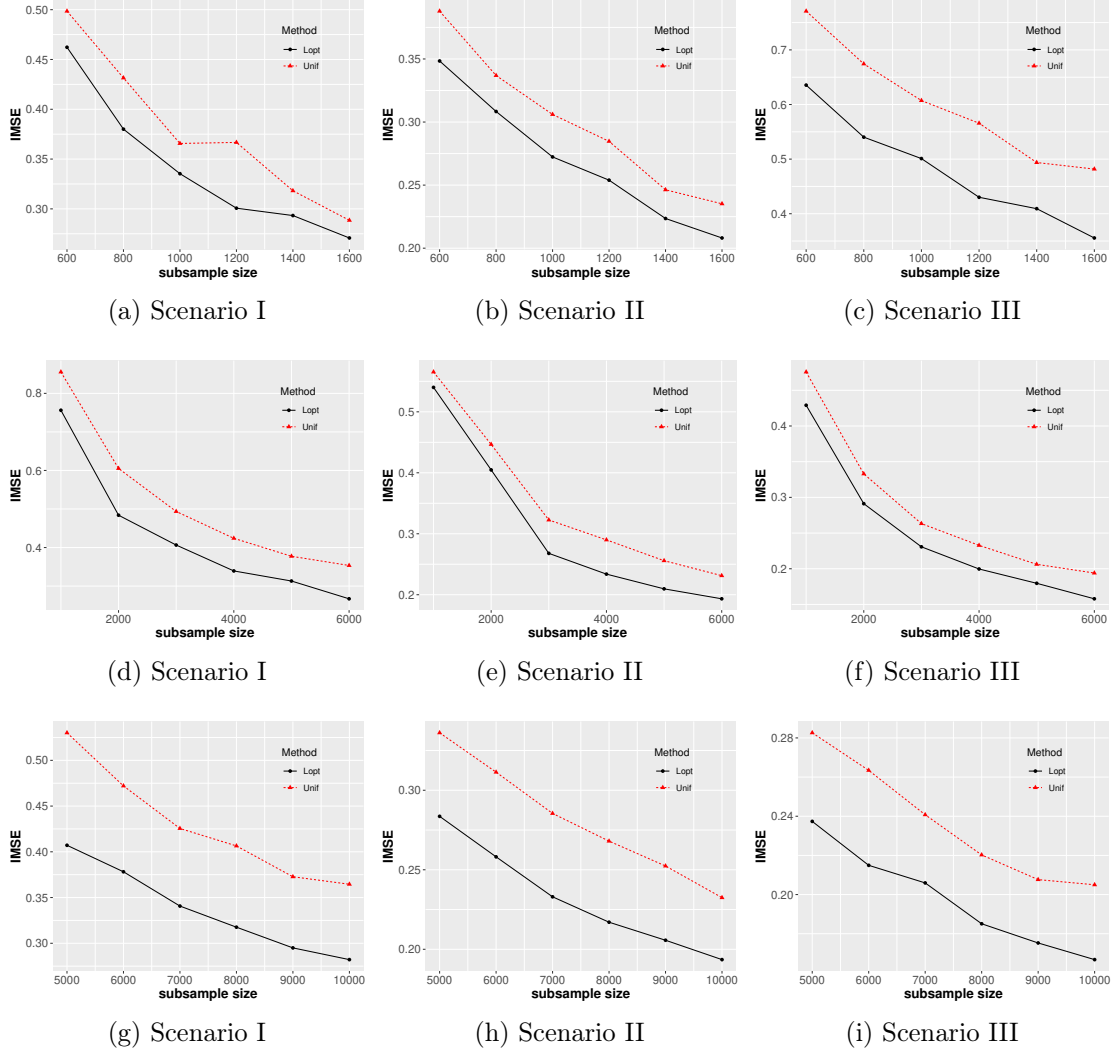


Fig. 8: When the response $y(x) \sim \text{Poisson}(\lambda(x))$, (a)-(c) show the IMSEs for different subsample sizes L and different scenarios under the full data size $n = 10^5$, (d)-(f) show the IMSEs for different subsample sizes L and different scenarios under the full data size $n = 10^6$, (g)-(i) show the IMSEs for different subsample sizes L and different scenarios under the full data size $n = 5 \times 10^6$.

likely that human activities caused more than half of the observed increase in global average surface temperature from 1951 to 2010. From the National Oceanic and Atmospheric Administration's (NOAA) Global Climate Report - Annual 2020 (<https://www.ncdc.noaa.gov/sotc/global/202013>), we can know that (1) the month of December 2020 had a global land and ocean surface temperature departure of 0.78°C above the 20th-century average—this was the smallest monthly temperature departure during 2020; (2) the month of December 2020 was the eighth warmest December on record; (3) with a slightly cooler end to the year, the year 2020 secured the rank of second warmest year in the 141-year record, with a global land and ocean surface temperature departure from average of $+0.98^\circ\text{C}$.

Besides, Global warming increases the severity of extreme rainfall and snowfall almost everywhere. A warmer world will increase soil evaporation and reduce the snow pack, exacerbating droughts even in the absence of reduced precipitation.

In this section, we use the global climate data set to analyze the change of temperature and precipitation in 1950, 2020, and 2100. RCP4.5 is a pathway labeled after a possible range of radiative forcing values at the end of the 21st century relative to pre-industrial values ($+4.5$ W per square meter), in which emissions peak in 2040. Because RCP4.5 is a more moderate scenario than RCP8.5 and RCP2.6, we choose to use the data based on it to analyze.

The daily precipitation, maximum and minimum temperature data under RCP4.5 are from the NASA Earth Exchange Global Daily Downscaled Projections (NEX-GDDP data set) (<https://ds.nccs.nasa.gov/thredds/catalog/NEX-GDDP/IND/BCSD/catalog.html>). In this data set, the globe is divided into 1,036,800 grids of 0.25 degrees \times 0.25 degrees using the Bias-Correction Spatial Disaggregation (BCSD). After deleting missing data, the full data size is $n = 1,028,032$ and $T = 365$. Fig. 9 (a)-(c) give the histograms of the log annual precipitation in different years and show that there is no obvious difference in the mean and median precipitation for different years. From Fig. 9 (d), we can say that the last century witnessed an increase in average temperature and in the future, the global average temperature will continue to increase.

Next, we want to study how the daily average temperature ($(\text{maximum} + \text{minimum})/2$, Celsius) through the whole year affects the log annual precipitation (mm) in 1950, 2020 and 2100, respectively. For each year, we use our proposed subsampling method (Lopt) and Unif method to fit a functional linear model:

$$\log(\text{Precipitation}_i) = \alpha + \int_1^{365} \text{Temp}_i(t)\beta(t)dt + \varepsilon_i, \quad i = 1, 2, \dots, 1028032.$$

Because we do know the true regression coefficient function, we consider using the empirical integrated mean square error (eIMSE) as the criterion for comparing different methods, where the eIMSE is defined by

$$\text{eIMSE} = S^{-1} \sum_{s=1}^S \int (\tilde{\beta}^{(s)}(t) - \hat{\beta}(t))^2 dt,$$

$\tilde{\beta}^{(s)}(t)$ is the estimator using the s -th subsample data, and $\hat{\beta}(t)$ is the estimator using full data.

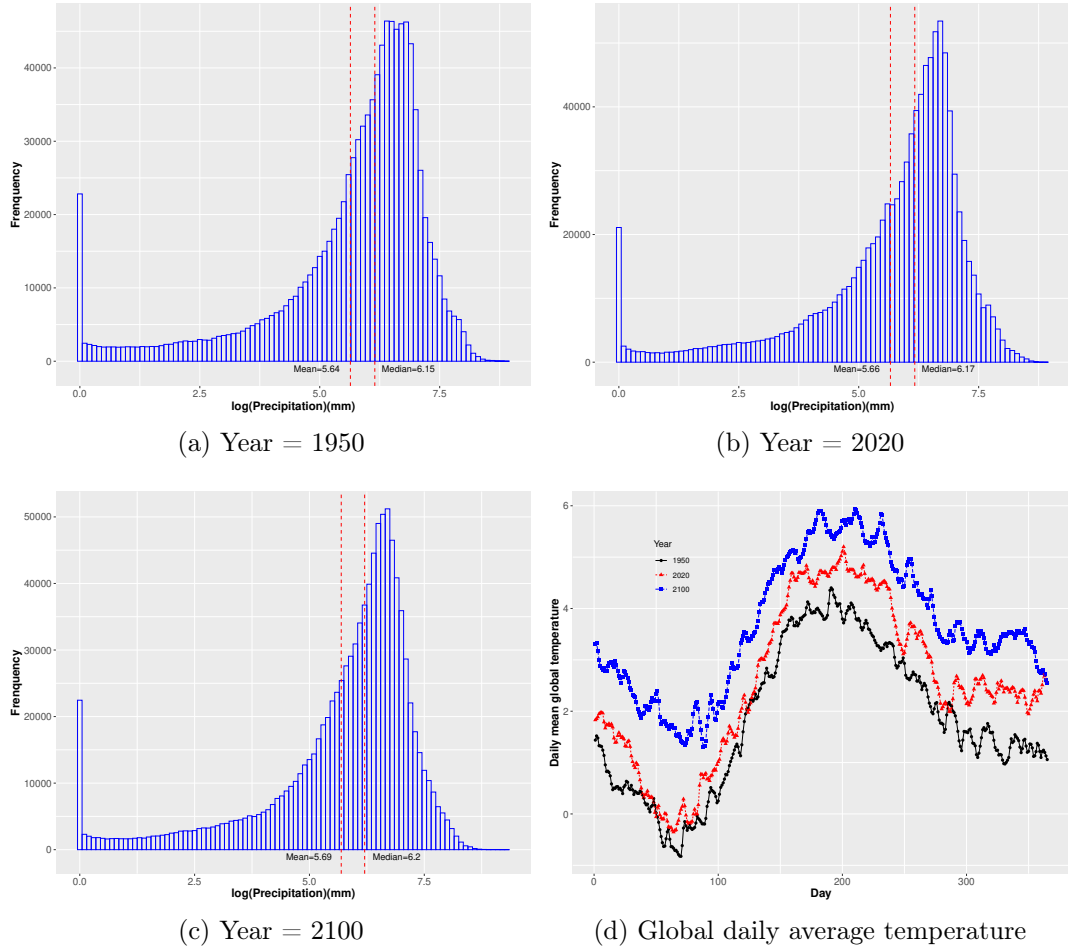


Fig. 9: (a)-(c) show the histogram of the log Annual Precipitation (mm) in the years of 1950, 2020 and 2100, respectively. (d) gives the global daily average temperature ($^{\circ}\text{C}$) in the years of 1950, 2020 and 2100.

Fig. 10 plots the selected samples with different methods for the data from 2020, and it shows that our method draws a random subsample based on the information of data, while the Unif method just uniformly randomly selects samples. Similar with the Simulation 5.1, we plot the eIMSEs for subsample size $L = 1000, 2000, 3000, \dots, 10000$ in Fig. 11. It is clear that in terms of eIMSEs, the Lopt method is better than the Unif method for the data in different years.

The averaged estimated coefficient functions using the Lopt method based on 1000 bootstrap samples with subsample size $L = 10000$ for predicting log annual precipitation (mm) from average daily temperature ($^{\circ}\text{C}$) are presented in Fig. 12. From this figure, it is obvious that the effect of temperature on precipitation is significantly different in different years. In 1950, there is a strong peak in the late fall and a strong valley in the winter. For 2020, there are two similar peaks in the late spring and late fall, while the coefficient decreases rapidly from late fall and reaches -3 at the end of 2020. In the future (2100), the coefficient function peak in the late spring and becomes minimum in May, which computes a contrast between spring and summer temperatures, with more emphasis on the spring. The corresponding 95% point-wise confidence intervals for different years are the shaded areas in Fig. 12, which indicated that the average daily temperature of the almost whole year has a significant impact on the annual precipitation.

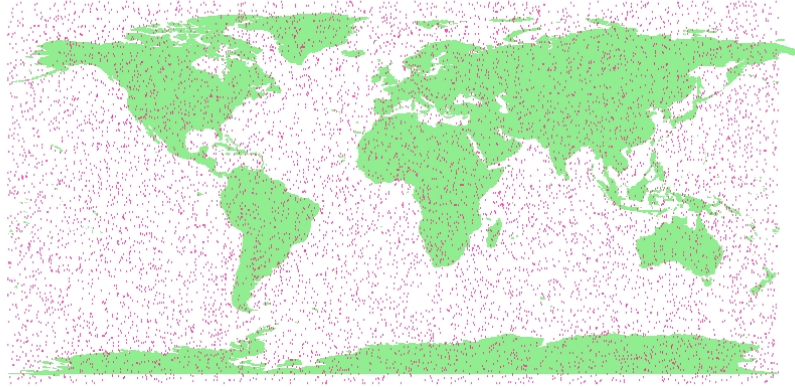
6.2. Kidney transplant data

The kidneys are a pair of organs in the human body, whose primary function is to remove waste from the body through the production of urine and regulate the chemical (electrolyte) composition of the blood. Renal failure means that the kidneys can no longer remove wastes and maintain electrolyte balance, which will threaten a human's life. Renal failure can be divided into acute renal failure and chronic renal failure. Regarding the treatment of chronic renal failure, one method is a kidney transplant. A successful kidney transplant can restore normal renal function to the patients and extend their survival time.

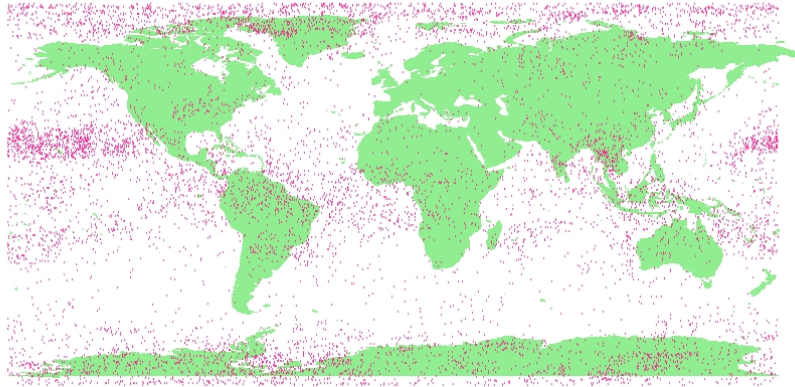
After kidney transplantation, kidney transplant recipients still face a high probability of losing transplant function. It is also important to follow up the graft function and predict the patient's expected lifespan after a kidney transplant. Creatinine is the waste product of creatine, which the muscles use to make energy. Typically, creatinine travels in the blood to the kidneys where it leaves the body in the urine. High levels in the blood might indicate that the kidneys are not working correctly. However, looking at how much creatinine is in the blood is not the best way to check how well the kidneys are working. That's because the level of creatinine in blood is affected by age, race, gender, and body size. (In other words, what's considered "normal" depends on these factors). The best way to know if kidneys are working properly is by looking at glomerular filtration rate (GFR) (Levey et al., 1999; Dong et al., 2018; Keong et al., 2016).

For adults ($\text{Age} \geq 19$), we use the Chronic Kidney Disease Epidemiology Collaboration (CKD-EPI, Levey et al. (2009)) equation to obtain the estimated glomerular filtration rate (eGFR, $\text{mL}/\text{min}/1.73\text{m}^2$). For child ($\text{Age} \leq 18$), we use the Schwartz formula (Schwartz et al., 1976, 1987, 2009) to estimate the glomerular filtration rate.

The data resource used in this section is kidney transplant data from the Organ Procurement Transplant Network/United Network for Organ Sharing (Optn/UNOS) as



(a) Uniform subsampling



(b) Subsampling based on the functional L-optimality criterion

Fig. 10: (a) shows the selected samples in the year of 2020 using Unif method and (b) shows the selected samples in the year of 2020 using Lopt method.

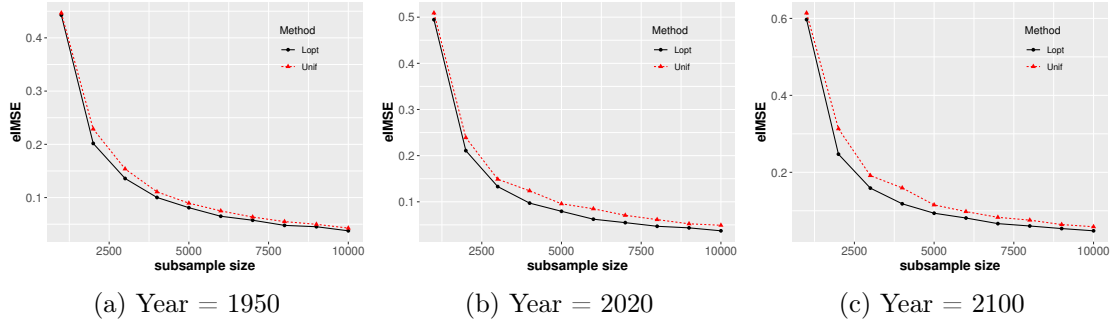


Fig. 11: A graph showing the empirical IMSEs for the global climate data set in the years 1950, 2020, and 2100, respectively.

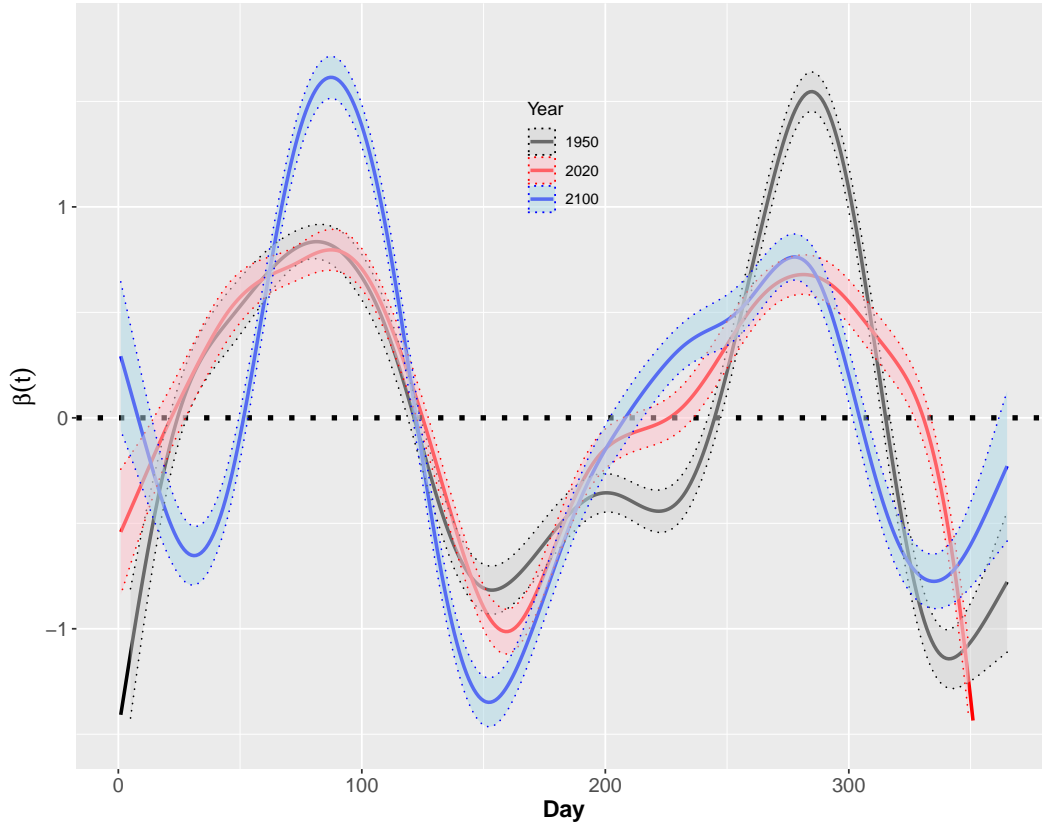


Fig. 12: The averaged estimated $\beta(t)$ using Lopt method based on 1000 bootstrap samples with subsample size $L = 10000$ for predicting log annual precipitation (mm) from average daily temperature ($^{\circ}\text{C}$) in the years of 1950, 2020 and 2100. And the shaded areas are the corresponding 95% point-wise confidence intervals based on the 1000 bootstrap samples with subsample size $L = 10000$.

of September 2020, which collect the basic description (e.g. age, race, gender, and height) of the kidney transplant recipients at the time of transplant and the information (e.g. serum creatinine, recipient status and the follow-up time) during the followed-up period. This data is available at <https://optn.transplant.hrsa.gov/> with the permission of OPTN/UNOS.

After matching data and deleting missing data, there are $n = 130313$ recipients who have lived for at least 5 years after kidney transplant. We divide these recipients into two categories, one is the category that the 30590 (23.3%) recipients die during the fifth to tenth year after the transplant ($Y = 0$), the other class is the 100713 (76.7%) recipients who have lived for at least ten years after transplant ($Y = 1$). It should be pointed out that we consider it as a dead case if a recipient needs to be re-transplanted. In Fig. 13, we display the eGFR curves for these two categories. From Fig. 13, it is obvious to see that the mean curve of $Y = 1$ is higher than that of $Y = 0$, which is consistent with the fact that the higher eGFR, the normal of renal function. And for those recipients who have not lived for ten years after transplant, the eGFR shows a significant downward trend. On the contrary, the eGFR curve remains stable for those recipients who have lived for ten years after transplant.

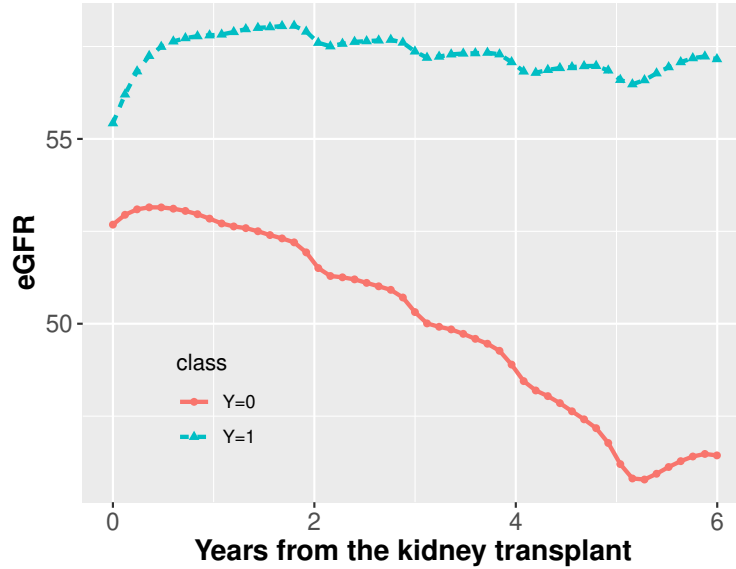


Fig. 13: The mean eGFR curves for two categories.

Next, we want to use the information of the kidney function (eGFR) in about the first five years after transplantation to predict lifespan. We consider fitting a logistic functional regression:

$$E(Y_i | \text{eGFR}_i) = \psi \left(\alpha + \int_0^6 \text{eGFR}_i(t) \beta(t) dt \right).$$

From Fig. 14 (a), it is obvious that the subsampling probabilities for different samples are very different. We plot the $\log(\text{eIMSEs})$ for subsample size $L = 2000, 2500, 3000, 3500, 4000, 4500$,

5000 in Fig. 14 (b). It is clear that in terms of eIMSEs, the Lopt method is better than the Unif method for the kidney transplant data.

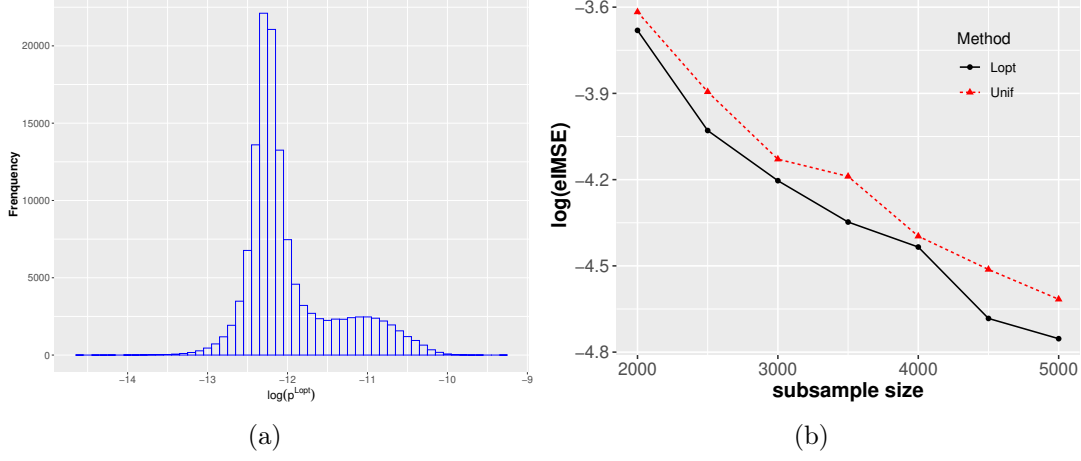


Fig. 14: (a) Histogram of the log of the subsampling probabilities p^{Lopt} . (b) The plot of the log empirical IMSEs for the kidney transplant data set with different subsample size.

The estimated coefficient function for predicting whether the recipient can live for at least 10 years after transplant based on the eGFR information in about the first five years is presented in Fig. 15. Fig. 15 respectively plots that the estimated coefficient functions based on $L = 5000$ random subsample data and full data, which shows these two curves are very close. This figure also gives the corresponding 95% point-wise confidence interval of the coefficient function based on 1000 bootstrap samplings with subsample size $L = 5000$, which indicates that only the coefficient from the fourth year after transplant is significantly non-zero. Therefore, we can use the information of eGFR during the fourth to the fifth year to predict the recipients' long-term lifespan, that is, whether a recipient can live beyond ten years.

7. Discussion

We propose the optimal subsampling algorithms motivated by the functional L-optimality criterion for the functional linear model and functional generalized linear model to tackle the challenges brought from the extraordinary amount of data. We also establish the asymptotic results of the subsample estimators obtained by these algorithms.

Simulation studies show that our proposed methods are computationally feasible and denote the uniform subsampling method for massive data. Our proposed subsampling methods are also used to analyze the global climate data and the kidney transplant data. In both applications, the results also show that the proposed subsampling method is better than the uniform subsampling method and can well approximate the results obtained by full data.

There is a challenging problem to be addressed in future research. For the extremely imbalanced data, our subsampling methods with replacement always select the same

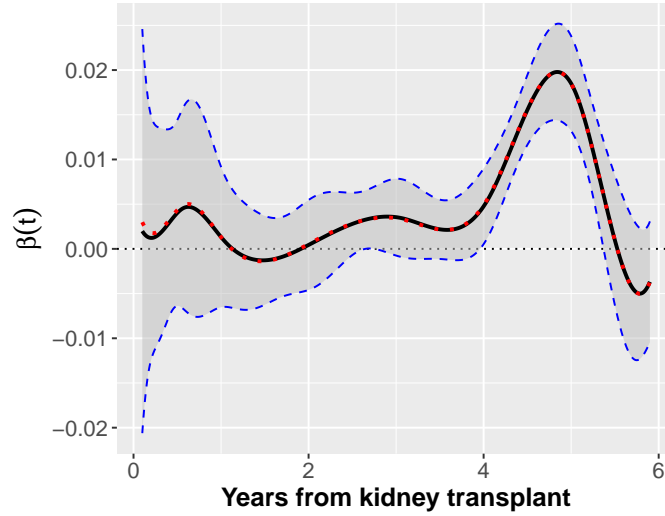


Fig. 15: The red dotted line is the estimated $\beta(t)$ based on the full data for predicting whether the recipient can live for at least 10 years after transplant based on the eGFR information in about the first five years. The black solid curve is the averaged estimated $\beta(t)$ using the Lopt method based on the 1000 bootstrap samplings with subsample size $L = 5000$. The blue dashed lines are 95% point-wise confidence limits on the curve based on the 1000 bootstrap samplings with subsample size $L = 5000$.

samples with very large subsampling probabilities and thus can not fit the data well. For this scenario, we will consider proposing a new subsampling method without replacement that will perform well for the extremely imbalanced data. In addition, for extreme weather, such as floods and droughts, we will consider a subsampling method in functional quantile regression.

References

- Ai, M., Wang, F., Yu, J., and Zhang, H. (2021a). Optimal subsampling for large-scale quantile regression. *Journal of Complexity*, 62:101512.
- Ai, M., Yu, J., Zhang, H., and Wang, H. (2021b). Optimal subsampling algorithms for big data regressions. *Statistica Sinica*. DOI:[10.5705/ss.202018.0439](https://doi.org/10.5705/ss.202018.0439).
- Atkinson, A., Donev, A., Tobias, R., et al. (2007). *Optimum Experimental Designs, with SAS*, volume 34. Oxford University Press, New York.
- Cardot, H., Ferraty, F., and Sarda, P. (1999). Functional linear model. *Statistics & Probability Letters*, 45(1):11–22.
- Cardot, H., Ferraty, F., and Sarda, P. (2003). Spline estimators for the functional linear model. *Statistica Sinica*, 13:571–591.

- Cardot, H. and Sarda, P. (2005). Estimation in generalized linear models for functional data via penalized likelihood. *Journal of Multivariate Analysis*, 92(1):24–41.
- Carroll, R. J., Fan, J., Gijbels, I., and Wand, M. P. (1997). Generalized partially linear single-index models. *Journal of the American Statistical Association*, 92(438):477–489.
- Chen, K., Hu, I., Ying, Z., et al. (1999). Strong consistency of maximum quasi-likelihood estimators in generalized linear models with fixed and adaptive designs. *The Annals of Statistics*, 27(4):1155–1163.
- Cheng, Q., Wang, H., and Yang, M. (2020). Information-based optimal subdata selection for big data logistic regression. *Journal of Statistical Planning and Inference*, 209:112–122.
- Claeskens, G., Krivobokova, T., and Opsomer, J. D. (2009). Asymptotic properties of penalized spline estimators. *Biometrika*, 96(3):529–544.
- Crainiceanu, C. M., Staicu, A.-M., and Di, C.-Z. (2009). Generalized multilevel functional regression. *Journal of the American Statistical Association*, 104(488):1550–1561.
- de Boor, C. (1978). *A Practical Guide to Splines*. Springer, New York.
- Dong, J. J., Wang, L., Cao, J., and Gill, J. (2018). Functional principal component analysis of gfr curves after kidney transplant. *Statistical Methods in Medical Research*, 27(12):3785–3796.
- Fan, Y., Liu, Y., and Zhu, L. (2021). Optimal subsampling for linear quantile regression models. *Canadian Journal of Statistics*, 0(0):1–19.
- Hall, P. and Horowitz, J. L. (2007). Methodology and convergence rates for functional linear regression. *The Annals of Statistics*, 35(1):70–91.
- Hilgert, N., Mas, A., and Verzelen, N. (2013). Minimax adaptive tests for the functional linear model. *The Annals of Statistics*, 41(2):838–869.
- James, G. M. (2002). Generalized linear models with functional predictors. *Journal of the Royal Statistical Society: Series B*, 64(3):411–432.
- Jiang, C. R. and Wang, J. L. (2011). Functional single index models for longitudinal data. *The Annals of Statistics*, 39(1):362–388.
- Jiang, F., Baek, S., Cao, J., and Ma, Y. (2020). A functional single index model. *Statistica Sinica*, 30:303–324.
- Keong, F. M., Afshar, Y. A., Pastan, S. O., Chowdhury, R., Binongo, J. N., and Patzer, R. E. (2016). Decreasing estimated glomerular filtration rate is associated with increased risk of hospitalization after kidney transplantation. *Kidney International Reports*, 1(4):269–278.
- Kiefer, J. (1959). Optimum experimental designs. *Journal of the Royal Statistical Society: Series B*, 21(2):272–304.

- Kim, M. and Wang, L. (2020). Generalized spatially varying coefficient models. *Journal of Computational and Graphical Statistics*. DOI:[10.1080/10618600.2020.1754225](https://doi.org/10.1080/10618600.2020.1754225).
- Levey, A. S., Bosch, J. P., Lewis, J. B., Greene, T., Rogers, N., and Roth, D. (1999). A more accurate method to estimate glomerular filtration rate from serum creatinine: a new prediction equation. *Annals of Internal Medicine*, 130(6):461–470.
- Levey, A. S., Stevens, L. A., Schmid, C. H., Zhang, Y., Castro III, A. F., Feldman, H. I., Kusek, J. W., Eggers, P., Van Lente, F., Greene, T., Coresh, J., and CKD-EPI (Chronic Kidney Disease Epidemiology Collaboration) (2009). A new equation to estimate glomerular filtration rate. *Annals of Internal Medicine*, 150(9):604–612.
- Li, T. and Zhu, Z. (2020). Inference for generalized partial functional linear regression. *Statistica Sinica*, 30:1379–1397.
- Li, Y., Wang, N., and Carroll, R. J. (2010). Generalized functional linear models with semiparametric single-index interactions. *Journal of the American Statistical Association*, 105(490):621–633.
- Liu, R., Yang, L., and Härdle, W. K. (2013). Oracally efficient two-step estimation of generalized additive model. *Journal of the American Statistical Association*, 108(502):619–631.
- Ma, P., Mahoney, M. W., and Yu, B. (2015). A statistical perspective on algorithmic leveraging. *The Journal of Machine Learning Research*, 16(1):861–911.
- McLean, M. W., Hooker, G., Staicu, A.-M., Scheipl, F., and Ruppert, D. (2014). Functional generalized additive models. *Journal of Computational and Graphical Statistics*, 23(1):249–269.
- Morris, J. S. (2015). Functional regression. *Annual Review of Statistics and Its Application*, 2(1):321–359.
- Müller, H.-G. and Stadtmüller, U. (2005). Generalized functional linear models. *Annals of Statistics*, 33(2):774–805.
- Pukelsheim, F. (2006). *Optimal Design of Experiments*. Wiley, New York.
- Ramsay, J. O. and Silverman, B. W. (2002). *Applied Functional Data Analysis*. Springer, New York.
- Schumaker, L. (1981). *Spline Functions: Basic Theory*. Wiley, New York.
- Schwartz, G., Haycock, G., Edelmann, C., and Spitzer, A. (1976). A simple estimate of glomerular filtration rate in children derived from body length and plasma creatinine. *Pediatrics*, 58(2):259–263.
- Schwartz, G. J., Brion, L. P., and Spitzer, A. (1987). The use of plasma creatinine concentration for estimating glomerular filtration rate in infants, children, and adolescents. *Pediatric Clinics of North America*, 34(3):571–590.

- Schwartz, G. J., Munoz, A., Schneider, M. F., Mak, R. H., Kaskel, F., Warady, B. A., and Furth, S. L. (2009). New equations to estimate gfr in children with ckd. *Journal of the American Society of Nephrology*, 20(3):629–637.
- Wang, H. (2019). More efficient estimation for logistic regression with optimal subsamples. *Journal of Machine Learning Research*, 20(132):1–59.
- Wang, H. and Ma, Y. (2021). Optimal subsampling for quantile regression in big data. *Biometrika*, 108(1):99–112.
- Wang, H., Yang, M., and Stufken, J. (2019). Information-based optimal subdata selection for big data linear regression. *Journal of the American Statistical Association*, 114(525):393–405.
- Wang, H., Zhu, R., and Ma, P. (2018a). Optimal subsampling for large sample logistic regression. *Journal of the American Statistical Association*, 113(522):829–844.
- Wang, L., Cao, G., et al. (2018b). Efficient estimation for generalized partially linear single-index models. *Bernoulli*, 24(2):1101–1127.
- Wang, L., Liu, X., Liang, H., and Carroll, R. J. (2011). Estimation and variable selection for generalized additive partial linear models. *Annals of statistics*, 39(4):1827.
- Xiao, L. et al. (2019). Asymptotic theory of penalized splines. *Electronic Journal of Statistics*, 13(1):747–794.
- Yao, F., Müller, H.-G., and Wang, J.-L. (2005). Functional data analysis for sparse longitudinal data. *Journal of the American Statistical Association*, 100(470):577–590.
- Yao, Y. and Wang, H. (2021). A review on optimal subsampling methods for massive datasets. *Journal of Data Science*, 19(1):1–22.
- Yu, J., Wang, H., Ai, M., and Zhang, H. (2020a). Optimal distributed subsampling for maximum quasi-likelihood estimators with massive data. *Journal of the American Statistical Association*. DOI:[10.1080/01621459.2020.1773832](https://doi.org/10.1080/01621459.2020.1773832).
- Yu, S., Wang, G., Wang, L., Liu, C., and Yang, L. (2020b). Estimation and inference for generalized geoadditive models. *Journal of the American Statistical Association*, 115(530):761–774.